Covalent Triazine Frameworks for Carbon Dioxide Capture

Han Wang, [a, b] Danni Jiang, [a, b] Danlian Huang, [a, b] Guangming Zeng, [* a, b] Piao Xu, [* a, b] Cui Lai, [a, b] Ming Chen, [a, b] Min Cheng, [a, b] Chen Zhang [a, b] and Ziwei Wang [a, b]

[a] College of Environmental Science and Engineering, Hunan University and Key Laboratory of Environmental Biology and Pollution Control (Hunan University), Ministry of Education, Changsha 410082, PR China;

[b] Key Laboratory of Environmental Biology and Pollution Control, Ministry of Education, Hunan University, Changsha 410082, P.R. China.

[*] Corresponding author at: College of Environmental Science and Engineering, Hunan University, Changsha, Hunan 410082, China. Tel.: +86–731– 88822754; fax: +86–731–88823701. E-mail address: zgming@hnu.edu.cn (G.M. Zeng) and piaoxu@hnu.edu.cn (P. Xu).

Abstract

Since the industrial revolution, the concentration of atmospheric greenhouse gases especially CO_2 released by human activity is increased year by year, leading to a series of serious problems such as global warming and climate change. Finding a way to mitigate this dilemma is of crucial importance. Covalent triazine frameworks (CTFs), as a new class of porous materials, have gain considerable attention due to their attractive chemical and structural merits. They show great potential for various applications especially for CO_2 capture. In this review, we aim to provide recent advances in using CTFs for CO_2 capture. First, a brief background is provided including a summary statement on the current situation of CO_2 issue, a general overview of typical porous materials used in CO_2 capture, and an introduction to CTFs. Second, synthetic reactions and methods related to CTFs are summarized and compared, and a short discussion of characterizations is provided. Further, CO_2 capture performance including CO_2 adsorption at low/high-pressure, gas selectivity, heat of CO_2 adsorption, recyclability and CO_2 capture of CTFs in a humid atmosphere are elucidated on the basis of CTF design. Then, strategies for enhancing the CO_2 adsorption ability of CTFs based on pore engineering and surface functionalization are given. Finally, a perspective of CTFs for CO_2 capture is presented.

1. Introduction

With the population growth and industrial development, one of the most serious problems facing the world is the global warming which has widespread influences on human and natural systems. According to data getting from National Oceanic and Atmospheric Administration (NOAA), the average global temperature of land and ocean surface in 2017 was 0.84 ℃ higher than that of twentieth-century (Figure 1a).[1] The increased emission of carbon dioxide (CO_2), mainly originating from the burning of fossil fuels in power plants or industrial manufacturing, is deemed as one of the chief culprits of the problem (Figure 1b). Thus, how to efficiently reduce the CO_2 emission is attracting considerable

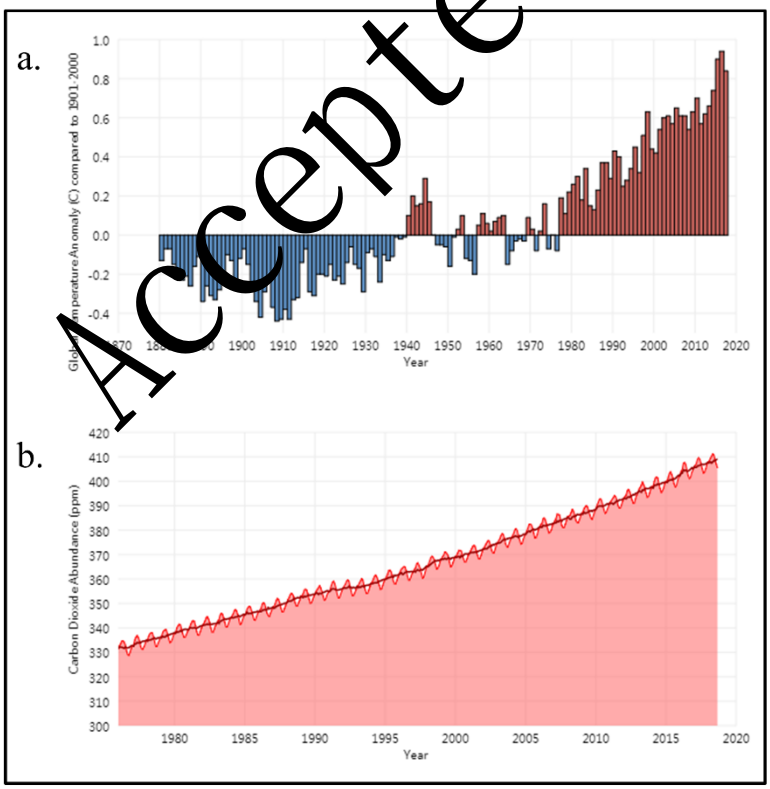

Figure 1. a. History of global surface temperature since 1880; b. Increased atmospheric CO_2 concentration measured during 1980-2017 at NOAA's Mauna Loa Observatory on Hawai'i. Reproduced with permission from ref. 1. Copyright 2017, NOAA Climate.gov.

attention. Carbon capture and storage (CCS) is widely regarded as a potential strategy to reach the target of CO_2 removal. Generally, a three-step CCS method including CO_2 capture, transportation and permanent storage is employed. While technologies of the CO_2 transportation and storage are widely studied and lots of them have reached the requirements of the commercialization, that of CO_2 capture is still far from being developed. The high cost and large energy penalty of CO_2 capture are impeding the deployment of CCS practical applications.

1.1. Technologies in CO_2 capture

Using clean energy with few or no carbon content like hydrogen technology is the best strategy, but it is still far away from sufficiently developed. Thus, reducing CO_2 generation from the source such as power plant and industrial operation seems to be the most direct way to lower the level of anthropogenic CO_2 in the atmosphere. Based on the emission of CO_2, several cost-effective and scalable technologies have been developed, namely pre-combustion capture, post-combustion capture, and oxy-fuel combustion (Figure 2).[2, 3]

Pre-combustion capture means a conversion before separating CO_2. O_2 or air is given to the system to react with primary fuel to produce H_2. Generally, the synthesis gas (syngas) composed of CO and H_2 is obtained because of the incomplete reaction. Hence, a shift converter, which enables the CO to further reacted with stream to produce CO_2 and involves more H_2, is needed and then it follows by various technologies to separate CO_2 and H_2.[4] While pre-combustion requires lower energy, the efficiency and temperature with respect to H_2-rich gas

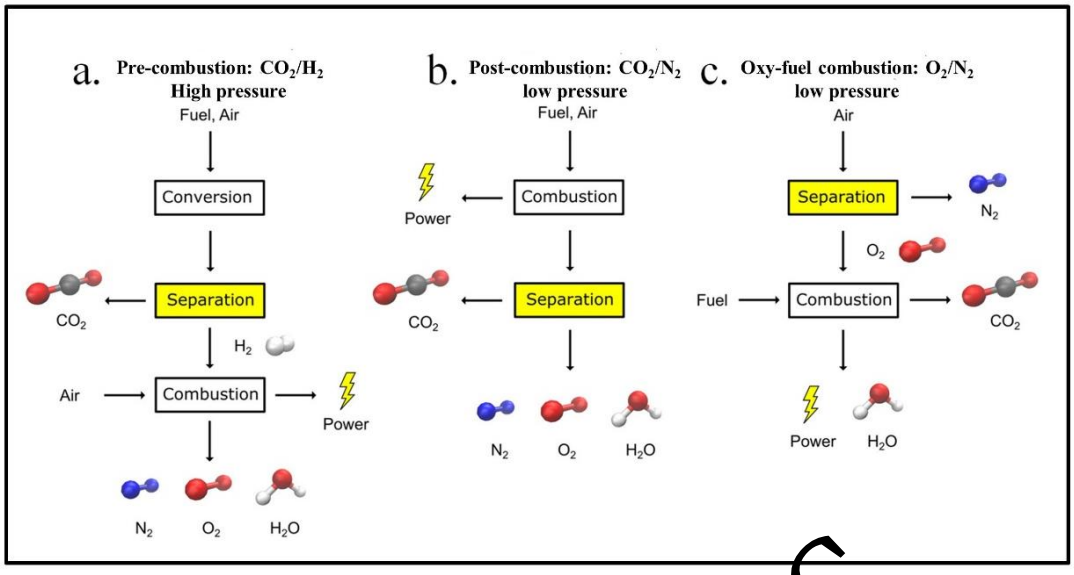

Figure 2. Representative scheme of CCS strategies: a. pre-combustion; b. post-combustion; c. Oxy-fuel combustion. Reproduced with permission from ref. 2. Copyright 2018, American Chemical Society.

turbine fuel might be a bit challenging. Moreover, the issues including the substantial capital cost and public resistance for new construction are also existed. Alternative methods such as chemical looping cycles need to be studied to generate syngas.[5]

Contrast to pre-combustion capture, post-combustion capture relies on the separation of CO_2/N_2 from exhaust flue gas before releasing to the atmosphere. The relatively low CO_2 concentration in combustion flue gas along with the atmospheric pressure and temperature of 40-150 ℃ make the process efficient.[6, 7] In addition, flue gases can be reused to the existing power plants by various technologies.[8] For example, bioreactors can be fed using cooled and CO_2-rich flue gases to produce microalgal biomass indicating that flue gases can be utilized as biofuel.[9-11] Furthermore, a unique strength of this technique is that the system

can continue to generate electricity in face of shutting down the CO_2 capture unit for an emergency.

Compared to the first two approaches, oxy-fuel combustion owns the advantage of producing almost pure CO_2 with almost pure O_2 instead of air to combust the fuels, which enables the direct storage.[12] But the deficiency of this approach is the essential prerequisite of pure O_2 that usually obtains from the air separation, which needs highly capital cost.

1.2. Materials in CO_2 capture

As mentioned above, the technologies of adsorption and separation for CO_2 capture seems to be the biggest challenge and sorbents with high performance are urgent to be designed and developed. Among the technologies used in CO_2 capture systems, chemical adsorption with aqueous amine solutions have reached the commercial criterion.[13] However, there are major drawbacks which greatly increase the running cost of power plants. For example, costly design for durability and frequent housekeeping for safe running are necessary considering that the amine solutions and vapors may cause equipment corrosion.[14] In addition, separating CO_2 from the sorbents needs a large quantity of energy, which also makes aqueous amine solutions uneconomical.[8]

Besides chemisorption, physisorption in porous materials has been considered as an attractive alternative because of its reversible process and smaller energy requirements. Several classes of porous materials including zeolites,[15, 16] porous carbons[17-20] and MOFs[21-24] are deemed to be promising

candidates in CCS applications as they have the merits of large CO_2 adsorption capacity, high CO_2 selectivity, good stability and regeneration. Moreover, mechanical robustness, pore size and pore surface engineering are important to consider. For example, zeolites, with low production cost, high thermal and chemical stability, high mechanical robustness and structural diversity, are regarded as strong candidates for CO_2 capture with good capacity and selectivity.[25] However, poor performance in humid conditions, high energy cost of regeneration, small high-pressure CO_2 capture capacity, and the difficulties in accurately functionalization and structure adjustment refrain the further development.[26] Activated carbons are another porous materials which have good high-pressure CO_2 capture capacity and retain high performance even in humid environment.[27-29] But major bottlenecks such as poor CO_2 selectivity, weak low-pressure working capacity, out-of-order pore width, and difficulties in pore engineering, greatly make their application be restricted. MOFs with great structure tunability and high porosity are identified as another ideal platforms for CO_2 capture.[30, 31] Compared to the above mentioned materials, characteristics such as capacity for pore functionalization give some MOFs relatively high CO_2 capture.[32-34] However, in some cases, the CO_2 capture performance of MOFs is closely correlated to its open metal sites, which preferentially bond with H_2O stronger than that of CO_2, and thus being unstable in humid gas mixtures. Peculiarly, even the MOFs with best performance have the challenge for

repeating uses in the present of water.[35, 36] In addition, their relatively weak mechanical robustness also impedes the practical application in CO_2 capture.[37]

1.3. Covalent triazine frameworks

As a newly emerging class of porous materials, covalent organic frameworks (COFs) have attracted much attention in the area of CO_2 capture.[38] On the one hand, COFs possess some similar performance with MOFs such as high CO_2 adsorption and selectivity, high structural tenability, and easy regeneration. On the other hand, COFs gain an advantage over MOFs because they can maintain the high CO_2 capture capacity in humid conditions. Covalent triazine frameworks (CTFs), are known as a subclass of COFs with triazine core, having been widely studies in CO_2 capture because of the nitrogen-rich nature. Interestingly, the discovery of CTFs may date back to 1978, while its growth was large after the year of 2008 with the work done by Kuhn and co-workers.[39] A series of CTFs with varied monomers was first systematically designed and constructed using ionothermal synthesis. Generally, CTFs are frameworks contained triazine units linked by covalent bonds which possess advanced stability compared to many coordinative-linked materials. The triazine unit can be formed in the trimeization reaction or simply originated from the building blocks. At the outset, CTFs were synthesized by trimeization reaction under ionothermal conditions with the catalysis of $ZnCl_2$. Soon after, some other construction approaches such as trifluoromethanesulfonic acid (TFMS) catalyzed condensation, Schiff-base

reaction, Friedel-crafts reaction have been introduced. Notably, the crystallinity of CTFs usually depends on the synthesis methods and conditions.

Different from above mentioned traditional crystalline porous solids, CTFs with precisely targeted, controllable and predictable synthesis are able to achieve pre-designable structural and chemical properties that specific to functions. In addition, they own high nitrogen content which can enhance the CO_2 capture by physisorption π systems. These along with the high surface area, tunable pore size, and low density endow them extremely widely scope of application potential especially in CO_2 adsorption. Specifically, in some cases, CTFs with ultra-high-surface-area show weak physical interactions with CO_2, and they have been used in pre-combustion carbon capture under the elevated pressures. The functional engineering of CTFs with polar groups, such as inorganic ions, oxygen-rich groups, and nitrogen-rich groups, can help to strengthen the average dipole-quadruple interactions with CO_2 molecules, thus improving the CO_2 capacity.

With the development of CTFs, while several reviews related to CTFs and their applications have been published,[40-42] the review specifically for the CO_2 capture is rare. In this review, a comprehensive summarization of CO_2 capture using CTFs is provided for the first time, and is classified as following sections based on the synthesis of CTFs and their application in CO_2 capture: (1) the synthesis reaction and conditions of CTFs are summarized containing trimerization reaction, Schiff-base reaction, Friedel-crafts reaction, nucleophilic

158 substitution reaction and so on; (2) the characterization of CO_2 capture
159 performance and the relationship between the chemical and structural natures of
160 CTFs and their adsorption capacities are provided; (3) strategies for enhancing
161 the CO_2 adsorption ability of CTFs are listed systematically including controlling
162 pore size and surface area, functionalization of pore wall and optimizing
163 technical procedure; (4) a brief conclusion and perspective for using CTFs for
164 CO_2 capture are also discussed regarding to the further development.

165 **2. Synthetic reactions and methods of CTFs**

166 One of the greatest strengths of CTFs is the tailor-made building blocks and
167 optional synthetic routes. To date, a significant amount of stable CTFs with
168 different topologies have been synthesized with various methods. Usually,
169 trimerization reaction catalyzed by $ZnCl_2$ or CF_3SO_3H is the most extensively
170 used method for the production of porous and stable CTFs. Nevertheless, other
171 reactions have also been utilized including Schiff-base reaction, Friedel-crafts
172 reaction, nucleophilic substitution reaction, Yamamoto coupling reaction and so
173 on. Herein the progress in the synthesis of CTFs is summarized.

174 **2.1. Trimerization reaction**

175 The vast majority of CTFs obtained via trimerization reaction have been prepared
176 under ionothermal conditions catalyzed by $ZnCl_2$ or trifluoromethanesulfonic
177 acid (TFMS). The molten $ZnCl_2$ salt in the reaction can act as solvent and catalyst

for the reversible cyclotrimerisation reaction, and strong Brønsted acids such as TFMS also can be used as catalyst related to the trimerization of nitriles.[43, 44]

2.1.1 $ZnCl_2$-based trimerization reaction

Early in 2008, Thomas and co-workers pioneered a way to synthesize porous CTFs via $ZnCl_2$-based trimerization reaction.[39] A series of nitrile building units, such as 1, 4-dicyanobenzene and 2, 6-dicyanopyridine, was employed to construct trimerization in the presence of molten $ZnCl_2$ at 400 ℃ to afford the black CTFs (Figure 3, taking CTF-1 as an example). The as-prepared CTFs showed high chemical and thermal stability. Usually, higher ratio of $ZnCl_2$ and monomers yields highly porous, yet amorphous materials.[45-49] And longer reaction time which enables the reversible and self-repairing formation of triazine rings leads to increased crystallinity.[50] However, only few crystalline CTFs have been reported using this approach, namely CTF-0,[50] CTF-1[39] and CTF-2[49] based on 1, 3, 5-tricyanobenzene, 1, 4-dicyanobenzene and 2, 6-dicyanonaphthalene monomers, separately. Several studies demonstrated that the carbonization would occur in the reaction process especially high temperature (400-600 ℃) and high $ZnCl_2$/monomer ratio, which caused the collapse of the structure and realized the extended pore apertures.[51, 52] Considering the high temperature about 400-700 ℃ and long reaction time like 20-116 h for the condensation of nitriles via conventional ionothermal conditions, Qiu and co-workers presented a microwave (MW)-enhanced ionothermal method for energy-saving and highly effective synthesis of CTFs.[53, 54] CTFs with high-surface-area could be obtained

easily in tens of minutes and higher MW power and longer reaction time led to higher BET surface area of CTFs with limits. Notably, all of the CTF materials synthesized under MW-assisted method were amorphous, and all the samples exhibited a type IV isotherm, indicating the structure of micropores with mesopores formed by the close-packed nanoparticles.[55] In this MW-enhanced synthesis, samples with high porosities (up to 2.52 cm^3/g) and surface area (up to 2390 m^2/g) could be easily realized within 10-60 min at a lower MW power output (280 W). To solve the problems that the thermal decomposition and acidolysis existed during the trimerization reaction and the $ZnCl_2$ catalyst was difficult to remove, Wang and co-workers further developed a consolidated ionothermal strategy to synthesis CTFs by the condensation of thermally unstable nitriles instead of the traditional one-step procedure.[56] Another similar strategy named multiple-step heating programs was applied to synthesize a series of porous triazine-based polyimide networks (TPIs@IC) which proved to be useful for synthesizing of CTFs from thermal/chemical unstable monomers.[57] For example, with the given molar ratio of $ZnCl_2$ and monomer (10:1), TPI-1@IC was synthesized by a selected temperature program (200 ℃/5 h, 300 ℃/5 h, and 400 ℃/20 h), while TPI-2@IC was obtained by a temperature program (200 ℃/5 h, 300 ℃/5 h, 400 ℃/10 h, 450 ℃/10 h, and 500 ℃/20 h). The BET surface areas of TPI-1@IC and TPI-2@IC was 1053 m^2/g, 814 m^2/g, separately, which was higher than that of TPI-1 (809 m^2/g) and TPI-2 (796 m^2/g) with the same chemical composition. Different from the reaction conducted in sealed vessels,

222 open crucible was used in a two-step approach that the first trimerization reaction
223 was run under lower temperatures and the next polymerization and crystallization
224 took place in the molten salt.[58] Pre-CTF was prepared in chloroform/TFMSA at
225 40 ℃. In further study, a molar ratio of 1 : 0.8 of pre-CTF to $ZnCl_2$ was employed
226 to realize CTF-$1_{(open)}$ while traditional CTF-$1_{(sealed)}$ obtained from a molar ratio
227 of 1 : 1 of monomer to $ZnCl_2$. After 40 h reaction time, the BET surface area of
228 CTF-$1_{(open)}$ was 910 m^2/g which was well comparable to that of CTF-$1_{(sealed)}$ (791
229 m^2/g).

230 **2.1.2. TFMS-catalyzed trimerization reaction**

231 Different from the black-colored products obtained via $ZnCl_2$-based
232 trimerization reaction, the CTFs synthesized under TFMS-catalyzed condition
233 show fluorescence characteristic which varied with building monomers. And the
234 TFMS-based trimerization is usually conducted in a mild condition, which

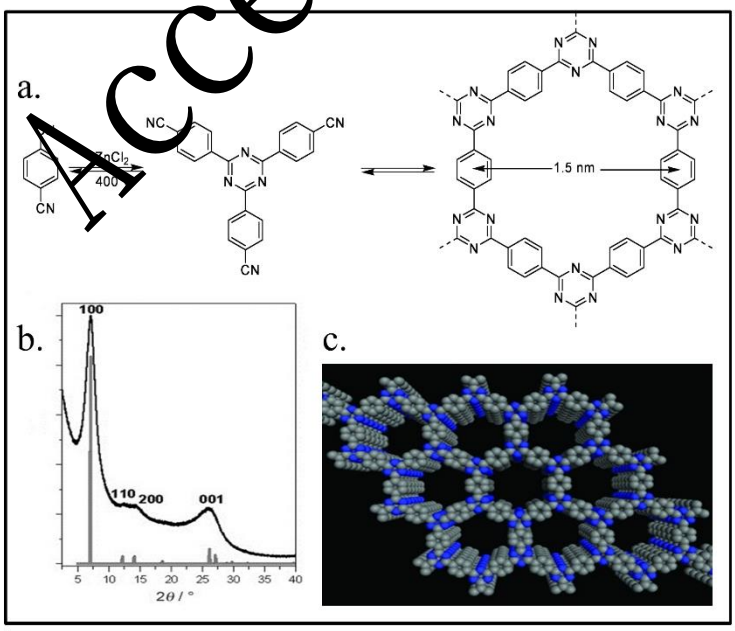

Figure 3 a. Representative synthetic routine of CTF-1; b. XRD pattern of CTF-1; c. structure of CTF-1. Reproduced with permission from ref. 39. Copyright 2008, Wiley-VCH.

enables the utilization of chemical and thermal unstable monomers. In 2012, Ren *et al*. synthesized P1-P6 and P1M-P2M via TMFS-catalyzed condensation under room temperature and microwave conditions, respectively.[59] The nitrogen content of P1-P6 and P1M-P6M was closer to the expected values than that of product obtained from ionothermal $ZnCl_2$-catalyzed synthesis, which means fewer overall defects. Notably, P1-P6 fabricated from room temperature showed amorphous structure, while P1M, P2M and P4M obtained via MW-assisted methods showed preferred orientation and limited crystallinity. In the MW-assisted reaction, the Brønsted acidic environment along with the increased pressure can facilitate the breaking and bonding of the triazine block at lower temperatures. Therefore, ordered domains can be formed through the thermodynamic function in the overall amorphous network. Moreover, the BET surface area of P2M-P6M were lower than that of P2-P6. Take P6 and P6M as representative examples, P6 was synthesized at room temperature while P6M was synthesized at 110 °C under the MW power output of 300W, which have the same backbone. The BET surface area of P6 (1152 m^2/g) was much higher than that of P6M (947 m^2/g). Similar results have been observed in other related studies such as some porous organic cages that lower porosity can be found in more ordered materials.[60] Subsequently, a tetraphenylethylene (TPE) based PCTF-8 was also prepared at room temperature by using TFMS as the catalyst.[61] This as-synthesized PCTF-8 exhibited photoluminescence behavior under UV light, while the sample synthesized at the high-temperature $ZnCl_2$-catalyzed

conditions did not show apparent emission due to the partial carbonization. Interestingly, F-CTF1 and F-CTF3 synthesized by TFMS-catalyzed method possessed high proportion of micropores while F-CTF2 synthesized under same conditions showed no porosity.[62] What is worth mentioning, porous F-CTF2 could be formed using the same monomer tetra(4-cyanophenyl)ethylene under ionothermal condition.[63] Similar result could be found that CTF-1 condensed from 1, 4-dicyanobenzene by ionothermal condition showed permanent porosity while P1 and P1M which have same chemical structure of CTF-1 showed no porosity.[39, 56, 59] There are two possible explanation that lead to the high porosity formed in $ZnCl_2$ ionothermal reaction: one is the template effect of $ZnCl_2$, and the other is the defects caused by the high temperature. Another modified one-pot solution synthesis of CTFs was presented as interface reaction by Xu and co-workers.[64] This method enabled the easy control of reversibility and the van der Waals epitaxial effect, which was conducive to the growth of two-dimensional polymer (2DP). Intriguingly, this reaction could be achieved in tens of minutes which was much fast than the abovementioned methods.

Different from liquid-phase reaction condition, CTFs based on cyclotrimerization of nitriles can be prepared under TFMS vapor atmosphere at elevated temperature (100 ℃) in solid phase synthesis (Figure 4).[65] Removable templates-silica nanoparticles (SiO_2 NPs) were employed to ensure the ordered and hollow nanostructure of CTFs, and the observation showed that there was no apparent collapse after removing the SiO_2 template, which was irreversible using

TFMS solution. Notably, the BET surface areas of the as-prepared CTFs were higher than that obtained from liquid phase synthesis. The authors further synthesized CTF-Th onto mesoporous silica SBA-15, which verified the universality of the method.[66]

Comparing the two trimerization reaction above, the advantages of TFMS-catalyzed trimerization reaction are obvious: (1) shorter reaction time and lower temperature; (2) avoiding the products contamination by extra $ZnCl_2$ catalyst; (3) eliminating undesired thermal decomposition and side condensation reaction such as carbonization and C-H bond cleavage and therefore decreasing framework defects. However, the strong acid nature of TFMS need to be taken into account.

2.2. Friedel-crafts reaction

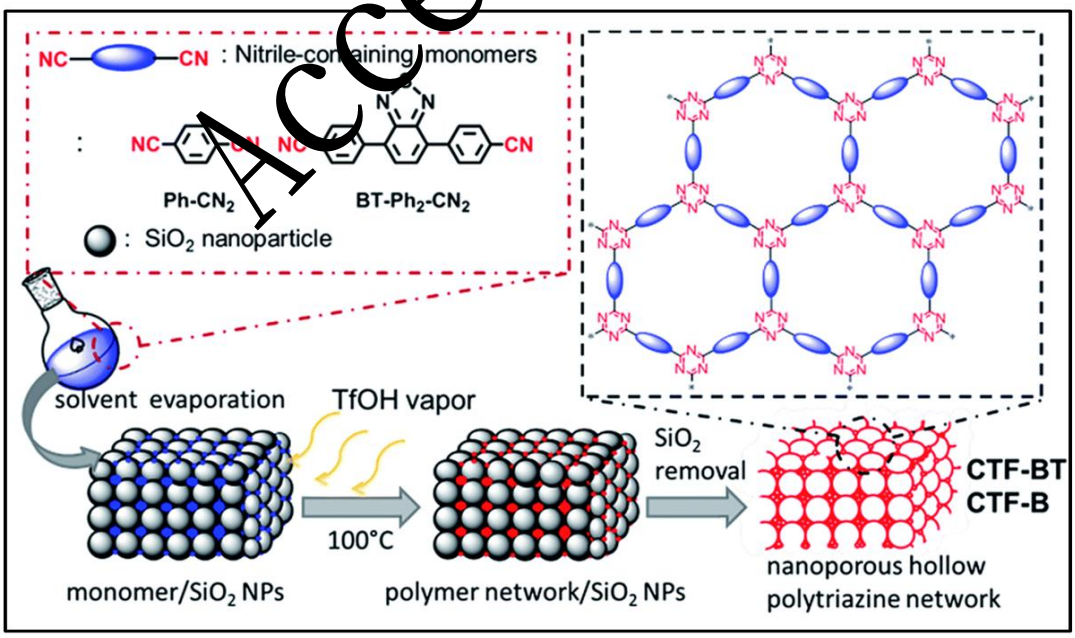

Figure 4 Scheme of solid phase synthesis and structures of CTF-BT and CTF-B. Reproduced with permission from ref. 65. Copyright 2016, Royal Society of Chemistry.

Cyanuric chloride (CC) with build-in triazine core is a qualified candidate in the synthesis of CTFs. Accordingly, a series of CTFs were synthesized via Friedel-Crafts reaction of CC with aromatic compounds.[67] CC was reacted with benzene (donated as polymer 2), biphenyl (donated as polymer 3), and terphenyl (donated as polymer 4) for 24 h under reflux in dichloromethane with the catalysis of $AlCl_3$, separately. The substitution reaction mainly occurred at the para-positions of the aromatic compounds. It was found that the accessible surface area is positively associated with the length of the aromatic linker. Polymer 3 and polymer 4 with increased length of the aromatic linker showed higher surface area. Similarly, four microporous CTFs based on CC with tri-, di-, and tetra-reactive units of 1, 3, 5-triphenylbenzene, trans-stilbene, and 1, 1, 2, 2-tetraphenylethylene / tetraphenylsilane were obtained via $AlCl_3$-catalyzed Friedel-Crafts reaction.[68, 69]

Methanesulfonic acid can also be used as the catalyst of Friedel-Crafts reaction. Xiong *et al.* and Das *et al.* polymerized triphenylamine with CC using methanesulfonic acid-catalyzed and $AlCl_3$-catalyzed Friedel-Crafts reaction, separately.[70, 71] One hand, methanesulfonic acid as a miscible liquid catalyst enabled the substantial improvement of the reaction efficiency and the products showed the fluorescent property. For another, the strong acid methanesulfonic acid in large excess (14 times excess) requires careful handing. Catalyzed by $AlCl_3$ is much milder and the products have a larger surface area.

Recently, an innovative mechanochemical approach was applied to synthesize CTFs via Friedel-Crafts reaction.[72] In the report, carbazole, acting as

electron-rich substrate, was selected to be a model monomer and employed as an activating agent along with the CC and $AlCl_3$. With the activating agent in stoichiometric amount and a bulking agent $ZnCl_2$, a planetary ball mill was used to mill then for 1 h to obtain a porous CTF. Compared to the CTFs obtained in ampoules, the materials prepared under the condition of ball milling possessed a higher C/N ratio, thus indicating no carbonization. Other monomers such as anthracene and triphenylbenzene were also utilized to prove the generality of this approach.

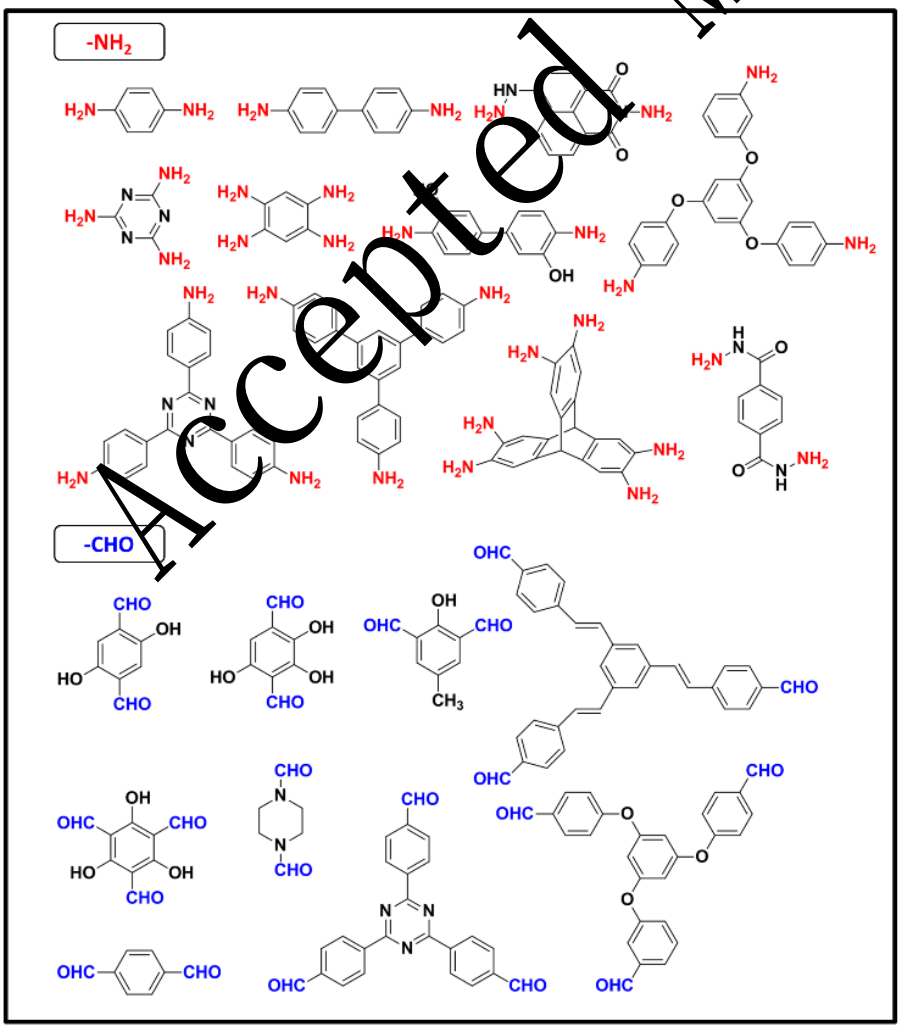

Figure 5 Building blocks bearing amine and aldehyde units involved in Schiff-base reaction.

2.3. Schiff-base reaction

Schiff-base reaction with reversible nature enables the formation of a crystalline framework. In addition, the possible utilization of diverse experimental conditions and various molecular precursors extends its feasibility and therefore the application in CTFs fabrication. Triazine-contained monomers with amino nodes, such as melamine,[73] 1, 3, 5-tris-(4-aminophenyl)triazine,[74] and 2, 4, 6-tris(4-aminophenoxy)-1, 3, 5-triazine[75] are well-suited for the synthesis of CTFs via Schiff-base chemistry (Figure 5). Mullen and co-workers prepared a series of SNWs via the Schiff-base reaction of melamine and di-/trialdehydes by heating monomers in dimethyl sulfoxide at 180 ℃ under inert conditions for 72 h.[76] The as-prepared materials showed high surface area and varied microporosity with different monomers. Moreover, as there is no catalyst used, the products are protected from contamination with inorganic remains. Later, Zhu and co-workers synthesized SNW-1 with same monomers but different synthesis condition.[77] The SNW-1 nanoparticles were obtained by the reaction of melamine and terephthalaldehyde under microwave conditions. Compared to the SNW-1 prepared from traditional solvothermal conditions for 3 days, the reaction time (6h) was dramatically reduced and the microporous framework with mesopores was formed via microwave method. In addition, 1, 3, 5-tris-(4-aminophenyl)triazine was used more than once to condense with aldehyde to obtain CTFs.[78, 79] Bhaumik *et al.* developed a triazine-based covalent organic polymer TRITER-1 from the condensation of 1, 3, 5-tris-(4-

aminophenyl)triazine and terephthaldehyde via Schiff-base reaction under the temperature of 150 ℃ for 12 h in anhydrous dimethylformamide under inert atmosphere.[80] Then, they further synthesized another CTF TRIPTA from Schiff-base condensation of 1, 3, 5-tris-(4-aminophenyl)triazine and 1, 3, 5-triformylphloroglucinol, which involved a reversible condensation and an inreversible keto-enol tautomerization.[81] Specifically, the reversible condensation aims to obtain highly ordered framework and the keto-enamine formation helps to maintain the high thermal and chemical stability.

Similarly, aldehydes with triazine core are also regular used related to CTFs.[82-86] Triazine-based benzimidazole-linked polymers (TBILPs), TBILP-1 and TBILP-2, were prepared by the polymerization of 2, 4, 6-tris(4-formylphenyl)-1, 3, 5-triazine (TFPT) with 1, 2, 4, 5-benzenetetraamine tetrachloride (BTA) and 2, 3, 6, 7, 14, 15-hexaaminotriptycene (HATT), separately.[87] The BET surface area of TBILP-1 and TBILP-2 was 330 m^2/g and 1080 m^2/g, separately. The introduction of triptycene core enables TBILP-2 to have high internal molecular free volume as well as low interpenetrated networks. In addition, Zhou and co-workers constructed a new triazine-based covalent organic polymer (COP-NT) by condensing naphthalene imide derivative and triazine derivative with the mixture of mesitylene, 1, 4-dioxane and glacial acetic acid under the condition of 120 ℃ for three days.[85] Interestingly, the as-prepared COP-NT showed amorphous feature reflected by the Powder X-ray diffraction (PXRD) pattern.

2.4. Nucleophilic substitution reaction

Besides in Friedel-crafts reaction, CC with triazine core is also favorable in nucleophilic substitution reaction. Each chloro group of CC can be substituted via reacting with nucleophiles such as alcohols, thiols and amines, and the number of substitutions can be varied by controlling the temperature and other related factors. Several CTFs were fabricated via nucleophilic substitution reaction based on CC.[88-90] Zhao *et al.* prepared a novel triazine-based porous organic framework PAF-6 based on CC, and piperazine acted as a linear linker.[91] The polymerization in the mix solution of THF and DIPEA was first conducted in the ice-bath for 4 h and then under the temperature of 90 ℃. The Fourier transform infrared spectroscopy (FT-IR) spectra of PAF-6 confirmed the substitution of three chlorine atoms. PAF-6 exhibited high stability in common organic solvents such as acetone and DMF, and showed a certain degree of crystallinity which was possibly because of the introduction of piperazine and the kinetically controlled nature of the polymerization. Bai *et al.* chose CC as a center node to react with targeted linker molecules including urea, thiourea and thiosemicarbazide) to synthesize a series of novel functional CTFs (donated as CCU, CCTU and CCTS, respectively).[92] The aromatic C-N stretching modes at 1551 cm^{-1} in FT-IR spectra indicated the presence of triazine unit in these as-prepared products. The products showed partially crystalline while disordered structures in the long distance. Similarly, Pitchumani *et al.* developed a kind of mesoporous covalent organic polymer (MCOP) based on 4, 4'-

dihydroxybiphenyl and CC, which showed partial crystallinity and a certain degree of order.[93]

Patel *et al.* synthesized COP-3 via a conventional nucleophilic aromatic substitution that 1, 3, 5-benzenetrithiol reacted with triazine-contained CC losing the three destabilized chlorides to form R-S-R bonded networked insoluble mass.[94] In details, DIPEA was added to the mixture of 1, 3, 5-benzenetrithiol and 1, 4-dioxane at 15 ℃. And CC was dissolved in 1, 4-dioxane and then dropwise added to the solution of DIPEA, 1, 3, 5-benzenetrithiol and 1, 4-dioxane with continuous stirring in an N_2 environment at 15 ℃. The as-prepared product was first stirred at 15 ℃ for 1 h and then at 25 ℃ for 2 h before being stirred at 85 ℃ for 21 h. Similarly, COP-4, COP-5 and COP-6 based on 1, 4-benzenedithiol, biphenyl-4, 4'-dithiol, 4, 4'-thiobisbenzenethiolwere were also prepared. The complete substitution of chloride from CC could be observed from FT-IR spectrum confirming the formation of sulfur bridged COPs. And COP-3 exhibited the highest BET surface area about 413 m^2/g.

2.5. Condensation reaction of amine with dianhydrides

A series of polyimide-contained CTFs were prepared via the polymerization of melamine and dianhydride monomers in dimethyl sulfoxide at 180 ℃ under inert conditions for 72 h.[95] The as-prepared polymers were amorphous while products synthesized by directly heating monomers showed acceptable crystallinities.[96] Similarly, condensation of melamine and perylene-3, 4, 9, 10-tetracarboxylic dianhydride (PTCDA)was achieved by the catalyst of Lewis acid

(zinc acetate and imidazole complex).[97] The obtained PI-network showed good thermal stability with a uniform ultramicropore size which were less than 6 Å. Recently, Pyromellitic dianhydride and 1, 3, 5-tris-(4-aminophenyl)triazine were polymerized in the mixture of mesitylene, NMP and isoquinoline under the temperature of 160 ℃ for 5 days.[98] The as-synthesized framework showed good thermal and chemical stability, and a BET surface area of 1484 m^2/g.

2.6. Other related synthetic methods

A porphyrin-based POP with triazine skeleton (named as TPOP-1) was condensed by 4, 4', 4''-(1, 3, 5-triazine-2, 4, 6-triyl)tris(oxy)tribenzaldehyde with pyrole under acid hydrothermal conditions (Figure 6a).[99] The porous framework of TPOP-1 with a BET specific surface area of 560 m^2/g was prepared as follows: first, the strong acid reaction medium enables the protonation of the aromatic aldehyde and then the electrophilic aromatic substitution at the pyrrole occurs, thus generating porphyrin centers with three free -CHO groups per triazine unit and subsequently further condensing with another pyrrole. The solid-state MAS-NMR and FT-IR spectrum confirmed the existence of porphyrin and triazine units in TPOP-1 (Figure 6b and c). Besides, amorphous TCMPs with 1,3,5-triazine node were developed via (A3 + B2) or (A3 + B3) Sonogashira-Hagihara cross-coupling reactions by using a 1.5 : 1 molar ratio of ethynyl to bromo functionalities, and employing DMF as a solvent.[100] Networks formed by A3 + B3 copolymerization (TCMP-0: 963 m^2/g, TNCMP-2: 995 m^2/g) had higher surface areas than those obtained from A3 + B2 reactions (TCMP-3: 691

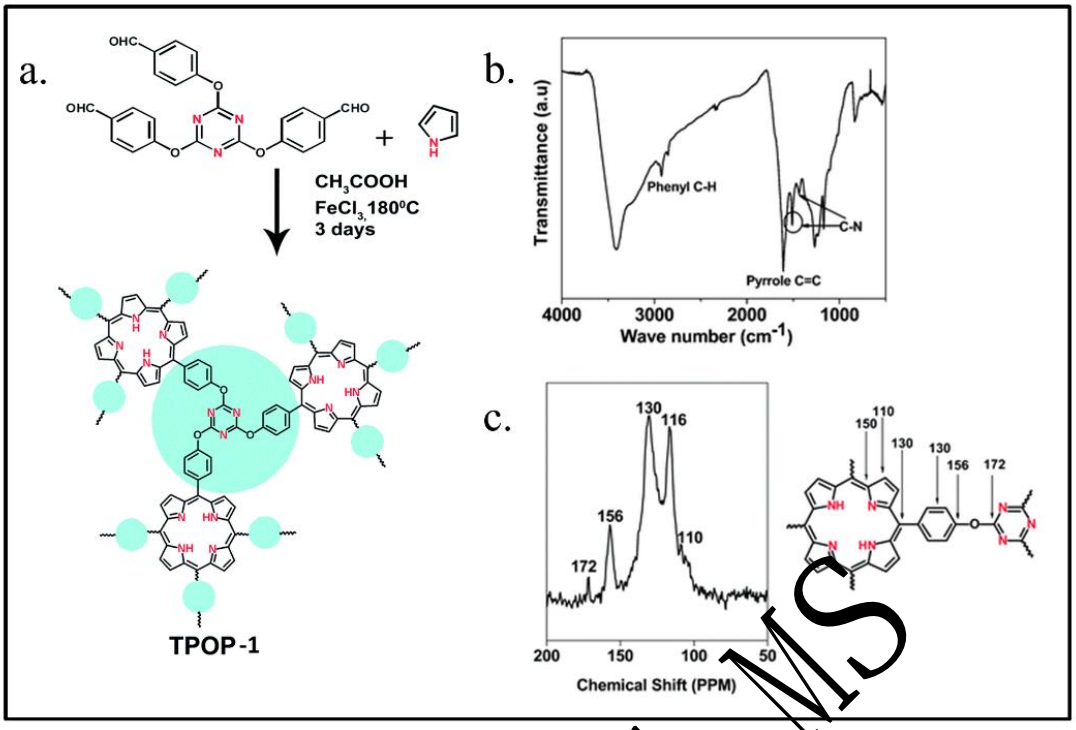

Figure 6 a. Schematic representation of the synthesis of Pd-TPOP-1; b. FT-IR spectrum of TPOP-1; c. Solid-state MAS-NMR of TPOP-1. Reproduced with permission from ref. 99. Copyright 2014, Royal Society of Chemistry.

m^2/g, TNCMP-5: 494 m^2/g). Zhang *et al.* developed a multifunctional carbazole-based conjugated microporous polymer MFCMP-1 based on 2, 4, 6-tris(carbazolo)-1, 3, 5-triazine by $FeCl_3$-promoted oxidative coupling polymerization.[101] The as-prepared MFCMP-1possessed a large BET surface area of over 840 m^2/g with a pore volume of 0.52 cm^3/g. And different from other COFs with crystallinity nature, it showed the amorphous nature.

In addition, other methods including Yamamoto coupling reaction, Stille cross-coupling polymerization have also been used to synthesize CTFs. For example, Ni-catalyzed Yamamoto reaction was employed by Cao and co-workers to synthesize a series of COPs based on tris(4-bromophenyl)amine, 2, 4, 6-tris-(4-bromo-phenyl)-[1, 3, 5]triazine, and 1, 3, 5-tris(4-

bromophenyl)benzene.[102] All the COPs possessed high BET specific surface area and high hydrothermal stability as well as graphene-like layer texture. Later, they further prepared a triazine-containing COP-T with hydrothermal stability by the self-coupling of 2, 4, 6-tris-(5-bromothiophen-2-yl)-[1, 3, 5]triazine (TBYT).[103] The characteristic peak at 512 cm^{-1} observed from the FT-IR spectra of COP-T was belongs to the C-Br stretching vibration, which indicated the complete Br elimination via phenyl-phenyl coupling in Yamamoto reaction. Gontarczyk and co-workers developed hybrid triazine-boron COF (BTA-COF-) by "one-pot" dehydration reaction.[104] Yu and co-workers fabricated pCTF-1 with triazine rings via the phosphorus pentoxide -catalyzed condensation based on aromatic amide rather than aromatic nitrile.[105] Kim and co-workers synthesizing a triazine-based covalent organic nanosheets with 2, 5-bis(trimethylstannyl)thieno-(3, 2-b)thiophene and 2, 4, 6-tris(5-bromothiophen-2-yl)-1, 3, 5-triazine (M2) through a Stille cross-coupling reaction.[106]

Recently, a new condensation strategy involving a Schiff base reaction followed by a Micheal addition was constructed for the reaction of aldehydes and amidines.[107] CTFs named as CTF-HUST-1, CTF-HUST-2, CTF-HUST-3 and CTF-HUST-4 were prepared at relatively low temperature (≤ 120 ℃) and ambient pressure which enabled the large scale synthesis. Later, the authors improved this strategy to obtain crystalline CTFs by slowing down the nucleation process through in-suit formation of aldehyde monomers by controlled oxidation of alcohol monomers.[108] The results demonstrated that CTF-HUST-C1 achieved

by alcohol oxidation strategy had better crystalline structure than the previous CTF-HUST-1. Generally, two steps are needed: at first the polymerization reaction occurs under a lower temperature for aldehydes formation controlling and then enhanced polymerization rate is maintained at a higher temperature for the improved crystallinity. And to further address the crystallinity issue, the same group developed a controlling feeding rate method to synthesize highly crystalline CTFs.[109] The nucleation process can be controlled by regulating the concentration with the feeding rate in an open system. According to this strategy, CTF-HUST-HC1 and CTF-HUST-HC2 were prepared which possessed better NO removal rate than amorphous CTF-HUST-1.

3. Characterization of CTFs

Characterization of CTFs is essentially similar to that of COFs, which concerns about atomic connectivity, structural regularity, morphology, and porosity. Powder X-ray diffraction (PXRD) is often used to analyse the structural regularity and the long range ordering.[48] Unfortunately, most of CTFs are amorphous, which makes the characterization quite troublesome and reveals limited information about the conformations. The atomic connectivity in CTFs, especially for the formations of linking bonds, is another important parameter for characterization. Solid-state nuclear magnetic resonance (NMR) spectroscopy, as a common but strong technique, has been well applied in other porous materials including zeolites[110] and MOFs,[111] which is undoubtedly useful in characterizing CTFs. Many atoms in the CTFs, e.g. ^{13}C, ^{1}H, ^{17}O, and ^{15}N, possess

the nuclear spin *I*, which endow them with NMR signal. For example, in the synthesis of CTF-CSU, NMR such as ^{13}C NMR and ^{1}H NMR is useful tools to confirm the structure of the corresponding precursors and intermediates.[112] Meanwhile, other characterization methods, such as elemental analysis (EA), infrared radiation (IR) and ultraviolet visible (UV-Vis) spectroscopies are also feasible, providing additional information on CTFs.[113] And thermogravimetric analysis (TGA) , as one of the most accessible method, can also not be neglected, which can provide first-hand information to investigate the thermal stability of CTFs.[114]

The surface area and porosity of CTF materials are normally assessed by gas (nitrogen or argon) adsorption-desorption measurements. For example, the porosity parameters of Tz-df-CTF materials were obtained by using the N_2 adsoption-desorption isotherm measured at 77 K.[115] The BET surface area was determined to be 1550 m^2/g for Tz-df-CTF400, 1878 m^2/g for Tz-df-CTF500, and 2105 m^2/g for Tz-df-CTF600, combining a total pore volume of 0.89, 1.08, and 1.43 cm^3/g, respectively. Scanning electron microscopy (SEM), transmission electron microscopy (TEM) and atomic force microscopy (AFM) are often used to probe the morphology, size and crystallinity. A representative example of the use was found in the study of CTF-HUST-HC1.[109] TEM, SEM, and AFM are utilized to analyse the morphology to reach the conclusion that CTF-HUST-HC1 possess a micrometer-size layered structure with and the thickness of 4.7 nm. HR-TEM images further revealed its highly crystalline nature. In addition, X-ray

photoelectron spectroscopy (XPS) is helpful to investigate the state of metal ions incorporated into the CTFs.[116]

Besides experimental studies, theoretical computation is an essential and useful auxiliary technique for investigating the structure and function of the frameworks. A majority of the theoretical research centers on the structure modelling of the CTFs, while others figure out the property and application prediction, such as hydrogen storage capability. Molecular modelling provides important information for the characterization and application of CTFs in predictive way. For example, in the study of Prof. Zhao, the electronic structure, work function, optical properties, and band edge alignment for monolayer and multilayer CTF have been investigated by using first-principle calculations.[117]

4. CO2 Capture Performance of CTFs

The successful structure and property design of CTFs inspired researches to investigate their performance in CO_2 capture. In recent years, studies on the application of CTFs in CO_2 capture have sprung up rapidly. The relevant surface area, pore parameters and CO_2 capacities of CTFs are summarized in the Table 1.[118-131] And to further illustrate the advantages and feasibility as well as the current limitations of CTFs for CO_2 capture, their CO_2 capture performance under different conditions is analyzed and discussed.

4.1. CO_2 adsorption at low pressures

CO_2 capture capacity is a significant criterion to judge the CO_2 capture performance of porous materials. The ability of CO_2 adsorption and selectivity at

low-pressure is very important for the effective separation of CO_2 in the process of post-combustion.[132] In low-pressure adsorption, the capacity performance depends more on CO_2-sorbent interaction than on surface area. Generally, CTFs with micropore less than 1 nm may show more effective CO_2 adsorption due to the molecular size of CO_2 (0.36 nm). For example, PHCTF-4 and PHCTF-6 had higher BET surface area than PHCTF-1a. And the V_{micro}/V_{total} value of PHCTF-1a, PHCTF-4 and PHCTF-6 was 79%, 58% and 39%, respectively, which means the more mesoporous structure of PHCTF-4 and PHCTF-6. The results indicated that the CO_2 adsorption capacities of PHCTF-4 (52.4 cm^3/g) and PHCTF-6 (51.9 cm^3/g) did not show significant difference from that of PHCTF-1a (51.9 cm^3/g), even though they have higher surface area.[124, 133] Therefore, designing uniform or ultra micropores CTFs is an effective means for improving the low-pressure CO_2 adsorption capability. Still, in addition to the comparative micropore volume, a larger surface area certainly can also offer the materials higher CO_2 adsorption capacity. Moreover, the surface functional group of the materials have a more significant effect. Compared to CTFs without polar groups on the pore wall, CTFs that have polar groups show more excellent CO_2 capture performance owing to the stronger interaction between CO_2 molecules and polar groups. The surface nature of CTFs plays a more important role at low pressure than the surface area. For example, FCTF-1 and FCTF-1-600 exhibited higher initial isosteric heat values of CO_2 adsorption (Q_{st}) value than that of CTF-1, CTF-1-600, which indicated that the introducing of C-F bonds indeed enhances its

affinity to CO_2 (Figure 7). Meanwhile, compared with CTF-1, CTF-1-600 possessed a smaller micropore surface area whereas a higher CO_2 adsorption. This may be because the nitrile groups in CTF-1-600 have stronger affinity to CO_2 then the nitrogen in CTF-1.[134] Interestingly, efficient doping of nitrogen might be able to obtain a higher CO_2 capacity then doping of oxygen.[135, 136]

4.2. CO_2 adsorption at high pressures

The performance of CO_2 adsorption at high pressure is very important for the purification of natural gas or the preparation of adsorbed natural gas (ANG) for future small-sized vehicles.[137, 138] different from the low-pressure adsorption mentioned above, high-pressure adsorption by CTFs are greatly determined by the surface area as well as pore volume. Usually, the CO_2 capture capacity increases with the higher surface area and pore volume due to the multi-layer

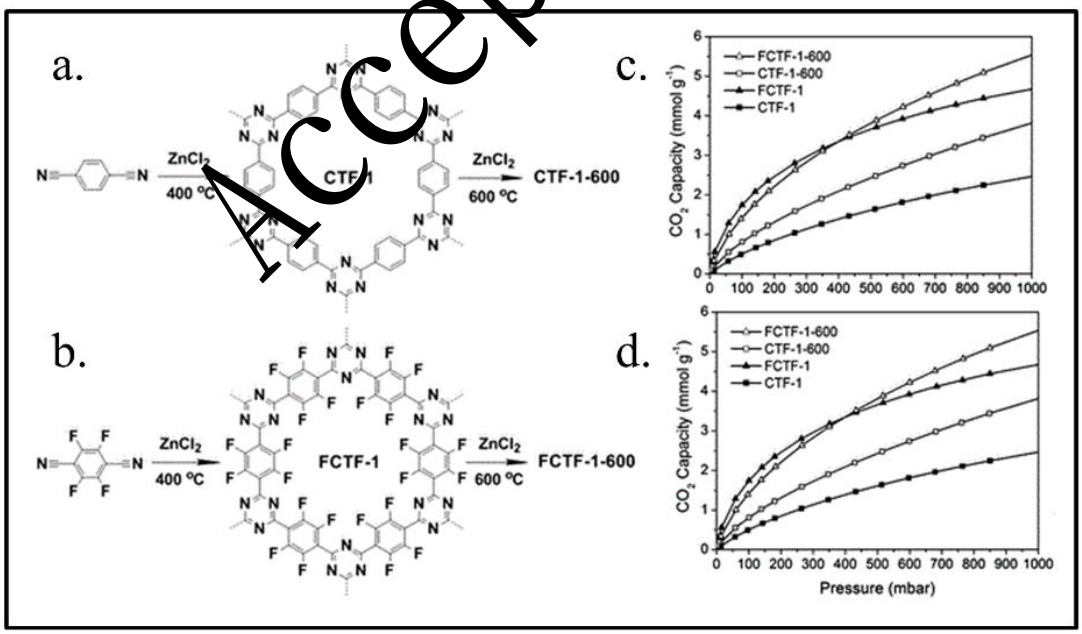

Figure 7 Reaction schemes and structures of CTFs synthesized through the trimerization of (a) terephthalonitrile and (b) tetrafluoroterephthalonitrile; c. CO_2 adsorption isotherms at 273 K; d. CO_2 adsorption isotherms at 298 K. Reproduced with permission from ref. 134. Copyright 2013, Royal Society of Chemistry.

adsorption under high pressure. Higher CO_2 adsorptions was achieved by MCTP-1 with higher surface area than that of MCTP-2 at 300K and 35 bar, respectively.[139] The CO_2 adsorption capacity of the CTF TRIPTA was tested under the condition of two different temperatures up to 5 bar pressure. With the increase of pressure, the amount of adsorbed CO_2 was on the rise and reached a maximum value 290.8 cm^3/g at 273K and 5 bar pressure. And TRIPTA can adsorb more CO_2 with the further increased pressure, considering that the isotherms did not reach any saturation value even though the rate of CO_2 adsorption was relatively slower in the high pressure region.[81] Similarly, the CO_2 adsorption of the polymer TRITER-1 showed the same trend at high pressure and reached a maximum value of 300 cm^3/g at 273K under 5 bar pressure.[80]

4.3. Gas selectivity and breakthrough performance

In addition to the adsorption performance, the gas separation is another important factor to assess the application of porous materials in CO_2 capture. And CCS related gas separation usually includes CO_2/H_2 separation, CO_2/N_2 separation, air (O_2/N_2), CO_2/CO and CO_2/CH_4 separation. Generally, selectivity is the main tool to weigh up the potential of CTFs in gas separation. In process of selective adsorption, two indicators need to be considered: adsorption capacity and selectivity. In most cases, single-component adsorption isotherms including Henry's law and Ideal Adsorbed Solution Theory (IAST) are used to calculate a material's selectivity. But this single-component adsorption calculations do not always involve all experimental variables as indicated by the name, thus the gas

586 mixture adsorption experiments like breakthrough experiments should also be
587 employed.[140] Lotsch and co-workers presented a series functional CTFs,
588 containing lutidine, pyrimidine and bipyridine building units, respectively, and
589 calculated the adsorption equilibrium selectivity of CO_2 and N_2 by the ratio of
590 the initial slopes in the Henry region and IAST at 298 K.[141] Pym-CTF500
591 possessed the highest selectivity (Henry: 189, IAST: 502), which outperforms
592 most CTFs measured so far, including FMAP-1 (Henry: 100, IAST: 107),[142] TPI-
593 2@IC (Henry: 69.6, IAST: 151),[57] and PCBZL (IAST: 148).[143] Notably, as the
594 increase of adsorption capacity, the selectivity decreases. This inverse
595 proportionality between adsorption and selectivity is a general trend in porous
596 materials chemistry.[144]

597 Generally, the breakthrough experiment is a way to evaluate the gas
598 separations performance of CTFs under kinetic flowing gas conditions in real
599 applications, which is more straightforward and reliable than single-component
600 isotherms for the calculation of selectivity, In the breakthrough experiment, the
601 compressed material is put in an adsorbent bed, and the mixture gas flows
602 through it. A gas chromatography or mass spectrometry is linked with the gas
603 outlet to analyze the composition of the outgoing gas streams. There are several
604 examples of breakthrough experiments for evaluating the performance of CO_2
605 separation in CTFs. Lai and co-workers evaluated the CO_2 separation
606 performance of several CTFs by breakthrough experiments. The experiments
607 were conducted separately, including CTPP using binary mixture of CO_2/N_2 at

298 K (Figure 8a and b),[145] TMCOP using steams containing CO_2/N_2 at ambient pressure and temperature (Figure 8c),[146] and CIN using CO_2/CH_4, CO_2/N_2 at 298 K (Figure 8d-f).[147] These CTFs have comparable or better CO_2 capture and separation performance compared to that of other porous materials in some cases. Other CTFs such as CTF-DCBT,[148] CTF-FUM and CTF-DCN[116] have also been tested by breakthrough experiments indicating that these CTFs can separate mixed gases of CO_2/N_2 and CO_2/CH_4 completely.

4.4. Heat of CO_2 adsorption

The heat of CO_2 adsorption (Qst) is used to analyze the interaction between CO_2 and the sorbent, which is an important parameter for CO_2 adsorption performance.

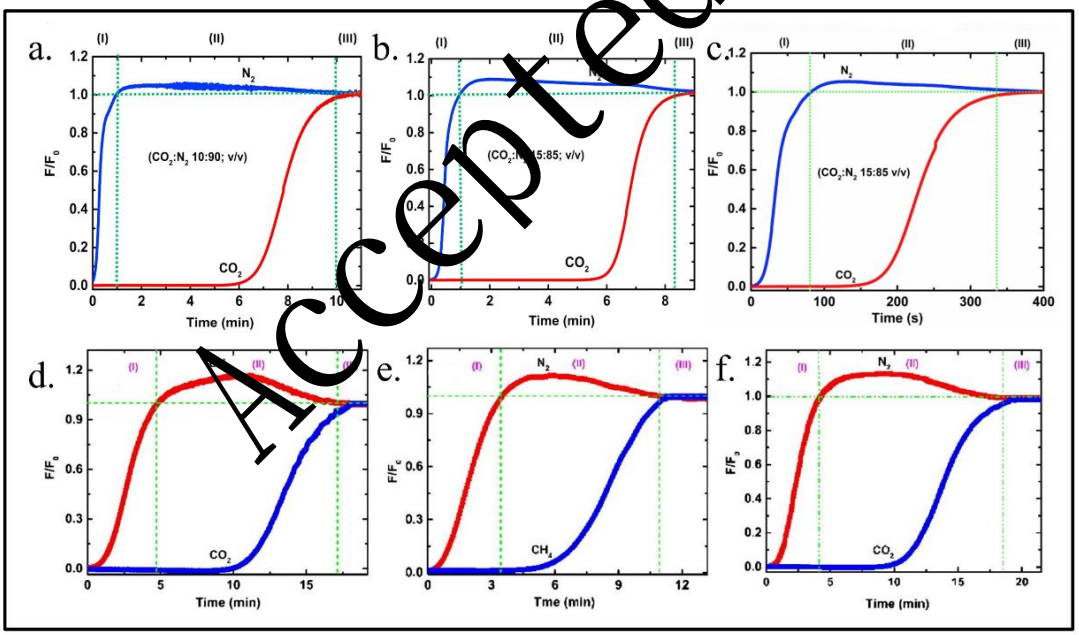

Figure 8 Column breakthrough experimental results for CO_2 and N_2 gas mixture at different feed gas compositions after activation by continuous He flow at 473 K for 12 h. (a) CO_2: N_2 (10: 90 v/v) and (b) 15: 85 measured at 298 K and 1 bar pressure of CTPP material. Reproduced with permission from ref. 145. Copyright 2016, Elsevier. (c) CO_2:N_2 (15:85 v/v) measured at 298 K and 1 bar pressure of TMCOP materials. Reproduced with permission from ref. 146. Copyright 2018, Elsevier. (d) CO_2:CH_4 (15:85 v/v), (e) CH_4:N_2 (15:85 v/v) and (f) CO_2:N_2 (15:85 v/v) measured at 298 K and 1 bar of CIN materials. Reproduced with permission from ref. 147. Copyright 2017, Elsevier.

Usually, Clausius-Clapeyron equation can be used to calculate the Q_{st} value can and first fitting the temperature-dependent isotherm can be used to evaluate for a virial-type expression.[149] For example, The Q_{st} value of CTF-DCN and CTF-FUM was calculated according to Clausius-Clapeyron equation from CO_2 adsorption isotherms at 298 and 273 K for investigating their binding affinity of for CO_2.[116] Q_{st} at zero coverage for CTF-FUM-350, CTF-FUM-400, and CTF-FUM-500 was 58.1, 55.0, and 50.3 kJ/mol, respectively, which is higher than that of CTF-DCN-400 (30.6 kJ/mol), CTF-DCN-500 (34.5 kJ/mol), TRITER-1 (38.1 kJ/mol),[80] and CTF-1 (39.6 kJ/mol).[150] The high nitrogen contents as well as the ultramicropore of CTF-FUM might be the reason of its high CO_2 binding affinities. In addition to weighing up the selectivity adsorption of CTF-FUM for CO_2, the Q_{st} values for N_2 and CH_4 of CTF-FUM were calculated with a result of about 9 and 25 kJ/mol, respectively. These lower Q_{st} values indicated the weaker interaction between N_2 (CH_4) and CTFs compared with that of CO_2, which means the high CO_2/N_2 and CO_2/CH_4 selectivity. Generally, the Q_{st} decreases with the increase of loading. And considering that the strong interactions may cause large energy consumption for the regeneration or desorption of the materials, high Q_{st} is not always necessarily good. What is worth mentioning that the Q_{st} values under 50 kJ/mol indicate that the physical adsorption of CO_2 is conducive to the regeneration.[133] The optimal Q_{st} values for separation are 30-50 kJ/mol.[151] In addition, the Q_{st} can be affected by the framework structure and pore size. CTF-py containing the pyridine units

possessed higher Q_{st} value (35.1 kJ/mol) than that of CTF-ph (33.2 kJ/mol) due to the Lewis acid-base interaction between CO_2 and the N-basic sites.[152]

4.5. CO_2 capture of CTFs in a humid atmosphere

Considering the inevitable moisture mixed in industry gases and natural gases in practical application, it is necessary to investigate the CO_2 capture performance of CTFs in a humid atmosphere. Understandably, the adsorption of water can cause materials degradation and sometimes the water molecule may compete against CO_2 for adsorption sites. For example, TBILPs with the covalent bonding nature were exceptionally stable in moisture and acids. However, these polymers provided binding sites for water due to the hydrophilic imidazole sites in the framework, which may have the influence on the CO_2 capture and selectivity.[87] Thus, designing and synthesizing materials with functional polar and basic groups preferring interactions with CO_2 as well as hydrophobicity would be an effective way. Ramanathan Vaidhyanathan and co-workers designed a triazine-resorcinol based porous polymer HPF-1 functionalized with polar phenolic groups.[153] According to the experiment results, HPF-1 lost only about 5% of the CO_2 adsorption capacity and had a CO_2/N_2 selectivity of 90:1 under the condition of a humid CO_2 stream. Notably, materials with high CO_2 adsorption originating from the nitrogen-rich units may simultaneously increases the affinity with water, which is probably caused by hydrogen bonding.[154]

4.6. Recyclability

Recyclability is an important parameter considering the practicality and economic feasibility of CTFs in large-scale CO_2 capture application. Generally, recyclability often be investigated by the repeat experiments of CO_2 adsorption/desorption cycles and regeneration in the laboratory. It is easy to understand that to be an economically feasible process, an ideal adsorbent must have large CO_2 adsorption capacity as well as good selectivity of CO_2. On the other hand, the interaction between CO_2 and adsorbents cannot be too strong, so as to avoid extra drag in the regeneration process. Reproducibility of two CTFs named CTF-FUM and CTF-DCN was investigated by conducting the adsorption-desorption cycles at 298 ℃.[116] The results demonstrated that the adsorption was reversible and no obvious loss of activity was observed even after ten cycles, indicating the excellent recyclability of two CTFs without any other heat energy input. Another study showed that the reproducibility of CO_2 adsorption for TPOP-1 was high considering that less than 4.0 wt% decrease in CO_2 adsorption capacity was observed after five consecutive adsorption-desorption cycles.[155]

5. Strategies for enhancing the CO_2 adsorption ability of CTFs

The inherent characteristics of CTFs, such as various synthetic methods, tailored structure and tunable functionalization motivate us to investigate its CO_2 adsorption related quality. Generally, high adsorption capacity and selectivity are two primary consideration for the special adsorption of materials. Considering the CO_2 adsorption capacity and selectivity of materials, there are two factors

needed to be emphasized: (1) compared to the miropores and mesopores, narrow ultramicropores (<1 nm) are preferred in CO_2 adsorption because they could enhance the CO_2 molecule occupation in the consideration of CO_2 thermodynamic size; (2) suitable banding energy is needed for high adsorption and desorption performance. As for the former, controlling the pore size and surface area is of great importance. As for the latter, introducing polar functional units onto the pore surface via pre- and post-modification could be one of the common and effective strategies. In this section, several strategies including pore size and surface area control, pore wall functionalization and technical means optimization associated with adsorption capacity and selectivity are given for enhancing the CO_2 adsorption ability of CTFs.

5.1. Controlling pore size and surface area

Usually, the pore size and surface area are significant for the performance of adsorbent materials. The size dependent molecular sieve effect has been studied extensively in porous materials, and the kinetic separation of the porous materials is also correlated with adsorbent's pore size and surface area.[156] It is worth mentioning that how to achieve the equilibrium: the pore size should be small enough to interdict undesired gas while large enough to get through the targeted molecular. CTFs with easily controllable design and synthesis, have the advantages over traditional zeolites and other similar molecular sieves in regulating surface area and pore size for the gas adsorption and separation.

As mentioned above, generally, the CO_2 capacity depends more on the surface area and pore volume in relevance of high pressure. Though there are a few exceptions, such as CTF-BI-10 had a higher surface area but lower CO_2 adsorption compared to that of CTF-BI-4.[47] The thermal transition hardsphere diameters of CO_2 molecular is 3.6 Å. Pore size that close to diameters are preferred for CO_2 adsorption. Reaction methods and conditions are of great importance related to pore size and surface area of CTFs. The different reaction conditions including temperature and the amount of catalyst lead to different pore size distributions of CTFs even with the same starting monomer, thus resulting in apparent distinction in CO_2 uptake capacities. Demonstrated by Cooper and co-workers, higher surface areas were obtained through room temperature method than that of microwave-assisted method.[9] Similarly, in ionothermal reaction, the amount of monomers and temperature has considerable influence on the porosity and structure characters. In particularly study, heating up the reaction temperature from 400 to 500 ℃ when keeping other conditions the same, the as-prepared CTFs exhibited a higher surface area with higher CO_2 adsorption capacity.[157] As for Friedel-crafts reaction, the pore properties of the products are strongly dependent on the degree of polymerization that is mainly influenced by the reaction mixture concentrations.[70] Specifically, high system concentration is more favourable in a way to enhance the pore parameters as the concentration range investigated. Thus, the porous characters of the samples can be easily controlled by changing the reaction concentration. In addition, chemical

activation of materials is another promising strategy to obtain sorbents with high surface area. Using KOH as the activating reagent to transform CTFs into active carbons with high surface area is very promising for CO_2 capture.[158, 159] For example, microporous CTF-1 was activated by KOH at 700 ℃ to produce a chemical activated CTF-1 (donated as caCTF-1-700). Generally, KOH is entirely consumed when heating up to 700 ℃. The obtained caCTF-1-700 remarkably possessed pore deepening with a higher surface area of 2367 m^2/g, thus greatly enhancing the CO_2 adsorption capacities up to 134.9 cm^3/g at 1 bar and 273 K (Figure 9).[150] Likewise, KOH-activated porous materials aPCTP-3c with narrow micropore size distributions possessed a higher surface area (2271 m^2/g) and larger micro/total pore volumes (0.87/0.95 cm^3/g) than that of pristine porous

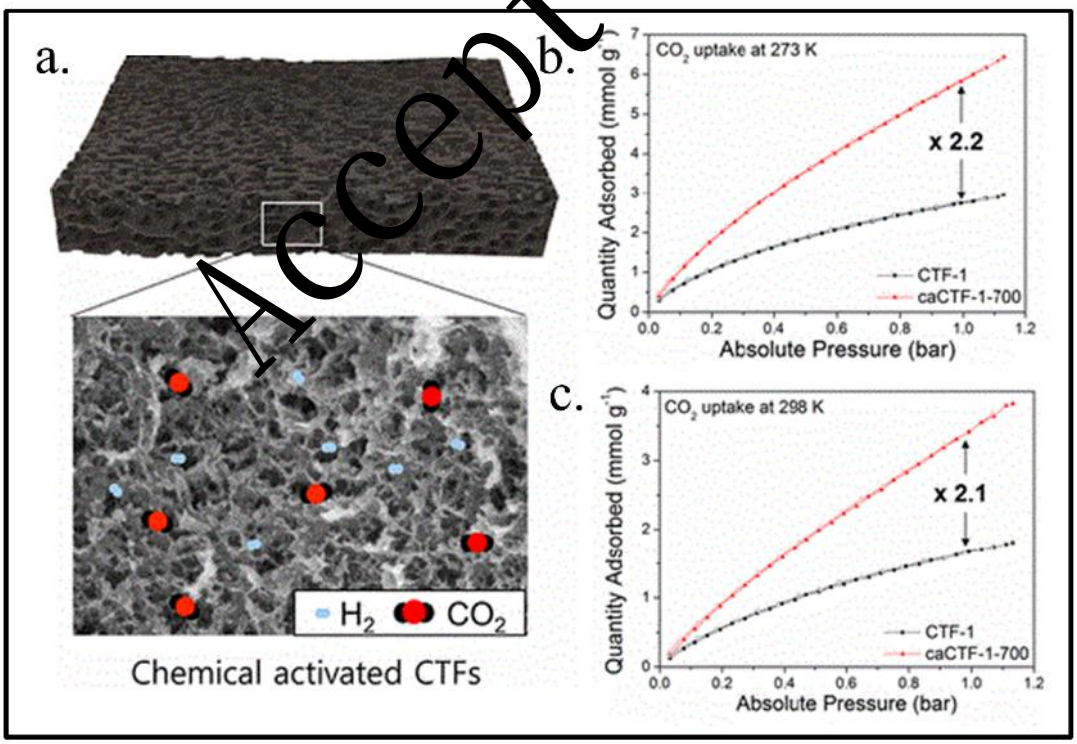

Figure 9 a. Schematic diagram of chemical activation CTFs; CO_2 adsorption–desorption isotherms measured at 273 K (b) and 298 K (c) for CTF-1 and caCTF-1-700. Reproduced with permission from ref. 150. Copyright 2017, American Chemical Society.

materials prepared without activation and the aPCTP-3c possessed higher CO_2 adsorption capacity of 144.8 cm^3/g at 273K and 1 bar.[160]

Ren *et al.* demonstrated that polymers originated from the more highly branched monomers exhibited higher surface area.[59] However, Gu *et al.* prepared four triphenylamine-based CTFs (PCTF-1 to PCTF-4).[154] The negative correlation between the BET surface area of PCTFs and branched arms revealed that higher density but lower surface area materials might be obtained from monomers with longer branches. As demonstrated by the authors, compared with PCTF-2, PCTF-4 just changed the middle benzene of the branches to benzothiadiazole, however, its BET specific surface area value and CO_2 adsorption capacity were the highest among the PCTFs. Besides, shortening and widening the size of monomer is another strategy to construct CTFs with ultramicropores. Zhong and coworkers synthesized CTF-FUM with short monomer fumaronitrile and CTF-DCN with wide monomer 1, 4-dicyanonaphthalene, respectively. As a result, ultramicropores nature was found in CTF-FUM (5.2 Å) and CTF-DCN (5.4 Å), and thus giving them remarkable adsorption capacity and selectivity for CO_2 over N_2 and CH_4.[161]

In addition to reaction methods and conditions, the size and structural features of building blocks can also affect the pore size. For example, CTF-0 with three functional groups of the 1, 3, 5-tricyanobenzene monomer has a smaller pore size than CTF-1, while CTF-2 has bigger pore size than CTF-1 due to its longer monomer (2, 6-dicyanonaphthalene). The pore size of the resulting CTFs

would be varied with the function groups on building blocks or the length of the building blocks.[162, 163] It is obvious that an increase in the BET surface area and micropore ratio in the CTF system can increase the CO_2 capture ability. In the study of Jürgen Senker, functional groups including triazines, imides, ethers, sulfones, and carbonyls had been employed to construct triazine-based polymers.[164] The results demonstrated that microporous TPI-1 with pore volumes of 0.44 cm^3 have the highest CO_2 uptake. Another study has revealed the relationship between CO_2 capture capacity with the building blocks' arm length. A series of CTFs was obtained from triphenylamine and monomers with varied branched arm lengths.[154] The as-prepared CTFs showed that the CO_2 uptake decreased with an increase in the arm length. In addition, the twisted and noncoplanar topology moiety is another choice to improve the porosity of CTFs. Phthalazinone structure-based CTFs had been designed with a high BET area of 1845 m^2/g and the CO_2 uptake up to 86.9 cm^3/g.[124]

5.2. Functionalization of the pore wall

CO_2 is a highly quadrupolar gas while the competitive sorbates commonly related to the CO_2 capture such as H_2, N_2, and CH_4 are weakly polar or even non-polar. This indicates that the interactions between these gases and materials are different which can be used to modify the pore surface characters of CTFs to enhance the performance of adsorption and separation. Generally, the surface characters of CTFs can be adjusted by pre-design of building blocks and functional sites doping as well as post-modification of existing CTFs.

780 Locating open active metal sites on the pore walls of CTF provides an
781 approach for enhancing adsorption of quadrupolar gases including CO_2, and
782 separation of non-polar gases including CH_4 and N_2. Liu *et al.* fabricated a class
783 of metal functional CTFs polymerized by metalloporphyrin.[119] An improvement
784 of the CO_2 adsorption capacity was observed due to the activated sites on the
785 pore wall that increases the interaction between materials and CO_2. This
786 enhanced adsorption depending on the open metal sites has also been favored in
787 FMAPs. Wang *et al.* constructed iron-decorated microporous aromatic polymers,
788 FMAPs, based on ferrocene and s-triazine monomers through Friedel-crafts
789 reaction.[142] FMAP-1 with a moderate BET surface area, showed higher CO_2
790 adsorption capability and more excellent IAST CO_2/N_2 selectivity than that of
791 ferrocene-free analogues.

792 Targeted introducing functional groups with strong CO_2 affinity into the
793 pores of CTFs is another effective way to enhance the CO_2 adsorption capacity
794 and selectivity. Zhao *et al.* designed a perfluorinated CTF (named as FCTF-1)
795 for selective CO_2 capture.[134] Thermodynamically, the electrostatic interactions
796 between the strongly polar C-F bonds and CO_2 molecules enhanced the CO_2
797 adsorption, especially at low pressures. Benzimidazole with secondary amine and
798 triazine groups shows CO_2-philic feature. CTF-BIs condensed from
799 benzimidazole containing monomers exhibited enhanced CO_2 adsorption
800 capability.[61] Remarkably, CTF-BI-4 and CTF-BI-11 showed higher CO_2
801 adsorption than CTF-0 derived from TCB,[50] TPI-1-7 containing imide group[164]

and many others.[123, 124] Another representative study conducted by Liu and co-workers showed that nitrogen- and oxygen-rich phthalazinone structure-based CTFs, PHCTFs, had strong CO_2 affinity and thereby the marked CO_2 adsorption capacity.[124] The high electric field on the surface of the framework created by the N, O and S atoms in PHCTFs leads to a remarkable affinity with quadrupolar CO_2 molecules. Especially, efficient doping of oxygen is conducive to enhance the CO_2 adsorption under high-pressure condition, while doping of nitrogen tends to achieve higher CO_2 adsorption at relatively low pressure.[56]

Similar to the porous organic polymer scaffolds, charged CTFs have been confirmed to have higher CO_2 adsorption and selectivity than neutral CTFs. Buyukcakir *et al.* reported the first charged CTFs, cCTFs, by ionothermal reaction based on the monomer cyanophenyl substituted viologen dication.[114] The results revealed that the CO_2 adsorption capacities of cCTFs were higher than those of previously reported CTFs with similar nitrogen contents and surface areas. Indeed, cCTFs with charge centers enabled extra electrostatic interaction with CO_2 molecules and thereby possessed unconventionally high affinity of CO_2, thus leading to prominently higher CO_2 adsorption capacity than their neutral counterparts.

Yu and co-workers compared the two conventional modification ways, including pre-designable and post-synthesis modification. The incorporating of functional units on to the pore wall was well-controlled by the anchor of acetohydrazides, ethyl ester or acetic acid for highly efficient CO_2 capture

824 (Figure 10).[165] Two CTFs, CTF-CSU36@pre and CTF-CSU37@pre, were
825 constructed by pre-designed appending acetic acid or acetohydrazide on the wall.
826 On the contrary, post synthesis modification could be achieved by simply
827 hydrolysis or hydrazide reaction of a carbazole-bridged triazine framework with
828 pendant ethyl ester (CTF-CSU20) to obtained CTFs with the surfaces anchored
829 acetic acid (CTF-CSU36@post) or acetohydrazide groups (CTF-CSU37@post).
830 According to the results, CTF-CSU37@post exhibited the highest CO_2
831 adsorption of 29 cm^3/g at 273 K, which originated from the vital function of acid-
832 base interaction. It is worth mentioning that much higher CO_2 adsorption
833 capacities were achieved in the post-modified samples compared to the pre-
834 designed ones, mainly resulting from the higher pore volume and the higher
835 content of appended functionalities of CTF-CSU36@post and CTF-
836 CSU37@post. The oxygen-rich or nitrogen-rich porous frameworks could

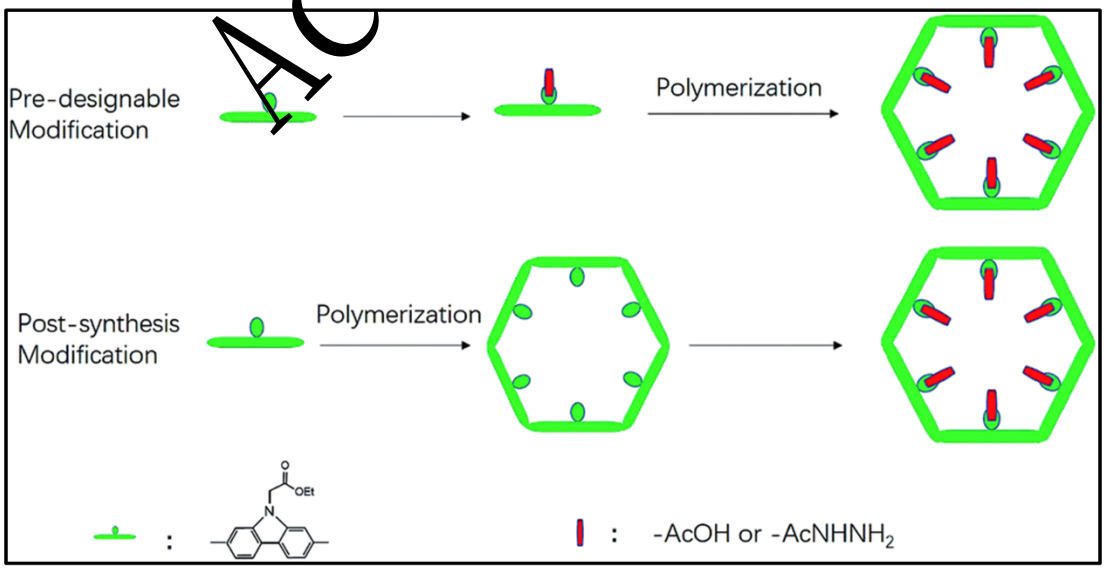

Figure 10 Schematic representation of pre-designable and post-synthesis strategies. Reproduced with permission from ref. 165. Copyright 2017, Royal Society of Chemistry.

indeed improve the host-guest interactions due to the enhanced dipole-quadrupole interaction.

5.3. Other technical means

Besides pore size and surface area control and pore wall functionalization, other technical means also can be employed and optimized to improve the CO_2 adsorption and separation capability in CTFs. With respect to the performance of CTF material in CO_2 capture, the follows can be utilized: (1) adjusting the morphological structure and dimensionality of CTFs, such as 3D architectures developed in high-pressure CO_2 adsorption; (2) Incorporating CTFs with other materials is also a powerful way to fabricate composites with new properties overmatching those of independent unites considering the synergetic effect and thus enhancing the performance; (3) generally, CTFs with different structure possess different CO_2 capture performance. It is necessary to select adsorption and separation methods according to the materials to optimize performance.

6. Conclusions

CO_2 capture has gain extensive attention in both science and technology field. Obviously, the performance of capture materials is the vital factor for any technology in CO_2 capture. CTFs, as a kind of newly emerging porous material, having the advantages of simple and easily available monomers, ease design and synthesis, and tailored functionalization, are potential for CO_2 capture. Although there have been a variety of synthesized and characterized CTFs that are used as

858 CO_2 capture materials, sufficiently developed and deliverable for real-application
859 is still in its shortage. Great efforts are essential to make for solving several
860 critical issues which will impede the development of CTFs for CO_2 capture if
861 they are not addressed.

862 (1) Only few crystalline CTFs have been reported. In most cases, the
863 amorphous property of CTFs causes poor accessibility of binding sites, and
864 therefore the fewer binding sites interact with CO_2 molecules in actual operation
865 than that of theoretically calculation. Moreover, it is hard to characterize the
866 amorphous CTFs even by PXRD, which disables to investigate the structure of
867 CTFs and thereby hamper the research of CO_2 capture mechanism. In addition,
868 CTFs are usually prepared in small quantities in laboratories. It can be difficult
869 to scale up in production. Without a workable process for scaling up, CTFs will
870 simply remain as niche materials with little values for large processing, including
871 carbon capture. Thus, new synthetic methods are still needed.

872 (2) Compared to the experimental studies, computational studies such as
873 molecular simulations and quantum calculations in this field need to be further
874 developed. Clearly, computational studies can be utilized to fund useful materials
875 as well as evaluate the relationships between structure and function and thus
876 providing guidance for the design and optimization of new CTFs samples. In CO_2
877 capture study, computational studies help to deciphering the potential of CTFs
878 for CO_2 capture, confirming the experimental results, digging deep into the
879 effects of structural changes, the role of pore size, and the molecular interaction

and transport mechanism. In this sense, combining the computational studies with experimental efforts has the great advantageous in the improvement of CTFs for CO_2 capture, which may save both money and time.

(3) To date, the investigations on CTF materials' tolerance to water are limited. In practical CO_2 capture, including pre-combustion capture and post-combustion capture, the gas streams always contain water and it is energy-consuming and even unrealistic to add extra process for water removal before separation. Thus, materials with excellent water-resistance are preferred in CO_2 capture. Addressing this issue should focus on studies not only about the physical adsorption of water into the pores of CTFs but also about the chemical adsorption of water to the active sites including open metal center. In addition, very little data on the influence of acid gases during CO_2 adsorption in CTFs has been reported, which also needs to be paid more attention in the future study. And it is clearly that the measurement of multi-component adsorption is more practical with respect to real application.

(4) In practical application, it is of great importance to evaluate the reversibility of the CO_2 capture materials, especially at ambient temperature and vacuum cycles, for energy-saving. However, comprehensive studies of reversibility are limited. It is challenging that the reversibility of the CO_2 adsorbents preforms well while the O_{st} of the adsorbents is 50 kJ/mol or more. In some cases, the accumulated O_{st} of the entire adsorption process seems to be very high which means the difficulty for regeneration. But considering each individual

adsorption process, adsorption taking place at different sites may still be reversible and it is possible for desorption in a sequential program.

Conflicts of interest

There are no conflicts to declare.

Acknowledgements

This study was financially supported by the National Natural Science Foundation of China (51709101, 51879101, 51521006, 51378190, 51278176, 51408206, 51579098, 51579096, 51809090 and 51508177), the National Program for Support of Top-Notch Young Professionals of China (2014), the Program for New Century Excellent Talents in University (NCET-13-0186), Scientific Research Fund of Hunan Provincial Education Department (521293050), the Program for Changjiang Scholars and Innovative Research Team in University (IRT-13R17), Hunan Provincial Science and Technology Plan Project (2018SK20410, 2016RS3026, 2017SK2243), the International S&T Cooperation Program of China (2015DFG92750), the Three Gorges Follow-up Research Project (2017HXXY-05)and the Fundamental Research Funds for the Central Universities (531118010226, 531107051080, 531107051161, 531107051205).

Notes and references

1. https://www.climate.gov/.
2. D. M. Reiner, *Nat Energy*, 2016, 1, 15011.
3. G. Kupgan, L. J. Abbott, K. E. Hart and C. M. Colina, *Chemical reviews*, 2018, 118, 5488-5538.
4. J. D. Figueroa, T. Fout, S. Plasynski, H. McIlvried and R. D. Srivastava, *International Journal of*

Greenhouse Gas Control, 2008, 2, 9-20.
5. A. J. Alvaro, I. L. Paniagua, C. G. Fernandez, J. R. Martin and R. N. Carlier, *Energ Convers Manage*, 2015, 104, 170-179.
6. L. K. G. Bhatta, S. Subramanyam, M. D. Chengala, S. Olivera and K. Venkatesh, *Journal of Cleaner Production*, 2015, 103, 171-196.
7. J. Wilcox, R. Haghpanah, E. C. Rupp, J. J. He and K. Lee, *Annu Rev Chem Biomol*, 2014, 5, 479-505.
8. R. S. Haszeldine, *Science*, 2009, 325, 1647-1652.
9. S. Nanda, S. N. Reddy, S. K. Mitra and J. A. Kozinski, *Energy Sci Eng*, 2016, 4, 99-122.
10. Y. Yang, C. Zhang, C. Lai, G. M. Zeng, D. L. Huang, M. Cheng, J. J. Wang, F. Chen, C. Y. Zhou and W. P. Xiong, *Adv Colloid Interfac*, 2018, 254, 76-93.
11. L. H. Zhang, J. C. Zhang, G. M. Zeng, H. R. Dong, Y. N. Chen, C. Huang, Y. Zhu, R. Xu, Y. J. Cheng, K. J. Hou, W. C. Cao and W. Fang, *Bioresource Technol*, 2018, 261, 10-18.
12. R. Stanger, T. Wall, R. Sporl, M. Paneru, S. Grathwohl, M. Weidmann, G. Scheffl mecht, D. McDonald, K. Myohanen, J. Ritvanen, S. Rahiala, T. Hyppanen, J. Mletzko, A. Kather and S. Santos, *International Journal of Greenhouse Gas Control*, 2015, 40, 55-125.
13. M. Bui, C. S. Adjiman, A. Bardow, E. J. Anthony, A. Boston, S. Brown, P. S. Fennell, S. Fuss, A. Galindo, L. A. Hackett, J. P. Hallett, H. J. Herzog, G. Jackson, J. Kemper, S. Krevor, G. C. Maitland, M. Matuszewski, I. S. Metcalfe, C. Petit, G. Puxty, J. Reimer, D. M. Reiner, E. S. Rubin, S. A. Scott, N. Shah, B. Smit, J. P. M. Trusler, P. Webley, J. Wilcox and N. Mac Dowell, *Energy & Environmental Science*, 2018, 11, 1062-1176.
14. M. T. Ho, G. W. Allinson and D. E. Wiley, *Industrial & Engineering Chemistry Research*, 2008, 47, 4883-4890.
15. S. J. Chen, M. Zhu, Y. Fu, Y. X. Huang, Z. S. Tao and W. L. Li, *Appl Energ*, 2017, 191, 87-98.
16. N. T. T. Nguyen, H. Furukawa, F. Gandara, H. T. Nguyen, K. E. Cordova and O. M. Yaghi, *Angew Chem Int Edit*, 2014, 53, 10645-10648.
17. G. Sethia and A. Sayari, *Carbon*, 2015, 93, 68-80.
18. A. E. Creamer and B. Gao, *Environmental Science & Technology*, 2016, 50, 7276-7289.
19. G. Singh, K. S. Lakhi, S. Sil, S. V. Bhosale, I. Kim, K. Albahily and A. Vinu, *Carbon*, 2019, 148, 164-186.
20. D. Saha and M. J. Kienbaum, *Micropor Mesopor Mat*, 2019, 287, 29-55.
21. S. Chaemchuen, N. A. Kabir, K. Zhou and F. Verpoort, *Chemical Society reviews*, 2013, 42, 9304-9332.
22. M. L. Ding, R. W. Flaig, H. L. Jiang and O. M. Yaghi, *Chemical Society reviews*, 2019, 48, 2783-2828.
23. Z. Hu, Y. Wang, B. B. Shah and D. Zhao, *Advanced Sustainable Systems*, 2019, 3, 1800080.
24. A. A. Olajire, *Renewable and Sustainable Energy Reviews*, 2018, 92, 570-607.
25. O. Cheung and N. Hedin, *Rsc Adv*, 2014, 4, 14480-14494.
26. D. Bonenfant, M. Kharoune, P. Niquette, M. Mimeault and R. Hausler, *Sci Technol Adv Mat*, 2008, 9, 013007.
27. M. Sevilla and A. B. Fuertes, *Energy & Environmental Science*, 2011, 4, 1765-1771.
28. J. Wei, D. D. Zhou, Z. K. Sun, Y. H. Deng, Y. Y. Xia and D. Y. Zhao, *Adv Funct Mater*, 2013, 23, 2322-2328.
29. K. He, G. Q. Chen, G. M. Zeng, A. W. Chen, Z. Z. Huang, J. B. Shi, T. T. Huang, M. Peng and L. Hu,

Appl Catal B-Environ, 2018, 228, 19-28.
30. Z. J. Lin, J. Lu, M. C. Hong and R. Cao, *Chemical Society reviews*, 2014, 43, 5867-5895.
31. A. Schneemann, V. Bon, I. Schwedler, I. Senkovska, S. Kaskel and R. A. Fischer, *Chemical Society reviews*, 2014, 43, 6062-6096.
32. M. L. Foo, R. Matsuda, Y. Hijikata, R. Krishna, H. Sato, S. Horike, A. Hori, J. G. Duan, Y. Sato, Y. Kubota, M. Takata and S. Kitagawa, *J Am Chem Soc*, 2016, 138, 3022-3030.
33. S. Krause, V. Bon, I. Senkovska, U. Stoeck, D. Wallacher, D. M. Tobbens, S. Zander, R. S. Pillai, G. Maurin, F. X. Coudert and S. Kaskel, *Nature*, 2016, 532, 348-352.
34. K. Sumida, D. L. Rogow, J. A. Mason, T. M. McDonald, E. D. Bloch, Z. R. Herm, T. H. Bae and J. R. Long, *Chemical reviews*, 2012, 112, 724-781.
35. K. Gedrich, I. Senkovska, N. Klein, U. Stoeck, A. Henschel, M. R. Lohe, I. A. Baburin, U. Mueller and S. Kaskel, *Angew Chem Int Edit*, 2010, 49, 8489-8492.
36. J. M. Yu and P. B. Balbuena, *J Phys Chem C*, 2013, 117, 3383-3388.
37. Y. Yang, Z. T. Zeng, C. Zhang, D. L. Huang, G. M. Zeng, R. Xiao, C. Lai, C. Y. Zhou, H. Guo, W. J. Xue, M. Cheng, W. J. Wang and J. J. Wang, *Chem Eng J*, 2018, 349, 808-821.
38. H. Wang, Z. T. Zeng, P. Xu, L. S. Li, G. M. Zeng, R. Xiao, Z. Y. Tang, D. L. Huang, L. Tang, C. Lai, D. N. Jiang, Y. Liu, H. Yi, L. Qin, S. J. Ye, X. Y. Ren and W. W. Tang, *Chemical Society reviews*, 2019, 48, 488-516.
39. P. Kuhn, M. Antonietti and A. Thomas, *Angew Chem Int Edit*, 2008, 47, 3450-3453.
40. P. Puthiaraj, Y. R. Lee, S. Q. Zhang and W. S. Ahn, *Journal of Materials Chemistry A*, 2016, 4, 16288-16311.
41. Y. Zhang and S. B. Jin, *Polymers-Basel*, 2019, 11, 31.
42. M. Y. Liu, L. P. Guo, S. B. Jin and B. E. Tan, *Journal of Materials Chemistry A*, 2019, 7, 5153-5172.
43. S. J. Ren, D. L. Zeng, H. L. Zhong, Y. C. Wang, S. X. Qian and Q. A. Fang, *J Phys Chem B*, 2010, 114, 10374-10383.
44. A. Ranganathan, B. C. Heisen and I. D. F. Meyer, *Chem Commun*, 2007, DOI: 10.1039/b706627a, 3637-3639.
45. P. Kuhn, A. Forget, J. Hartmann, A. Thomas and M. Antonietti, *Advanced materials*, 2009, 21, 897-901.
46. W. Wang, H. Ren, F. X. Sun, K. Cai, H. P. Ma, J. S. Du, H. J. Zhao and G. S. Zhu, *Dalton T*, 2012, 41, 3933-3936.
47. L. M. Tao, F. Niu, C. Wang, J. G. Liu, T. M. Wang and Q. H. Wang, *Journal of Materials Chemistry A*, 2016, 4, 11812-11820.
48. L. Zhao, S. Shi, M. Liu, G. Z. Zhu, M. Wang, W. Q. Du, J. Gao and J. Xu, *Green Chem*, 2018, 20, 1270-1279.
49. M. J. Bojdys, J. Jeromenok, A. Thomas and M. Antonietti, *Advanced materials*, 2010, 22, 2202-2205.
50. P. Katekomol, J. Roeser, M. Bojdys, J. Weber and A. Thomas, *Chemistry of Materials*, 2013, 25, 1542-1548.
51. P. Kuhn, A. Forget, D. S. Su, A. Thomas and M. Antonietti, *J Am Chem Soc*, 2008, 130, 13333-13337.
52. J. T. Jia, Z. J. Chen, Y. Belmabkhout, K. Adil, P. M. Bhatt, V. A. Solovyeva, O. Shekhah and M. Eddaoudi, *Journal of Materials Chemistry A*, 2018, 6, 15564-15568.
53. W. Zhang, C. Li, Y. P. Yuan, L. G. Qiu, A. J. Xie, Y. H. Shen and J. F. Zhu, *Journal of Materials*

Chemistry, 2010, 20, 6413-6415.
54. W. Zhang, F. Liang, C. Li, L. G. Qiu, Y. P. Yuan, F. M. Peng, X. Jiang, A. J. Xie, Y. H. Shen and J. F. Zhu, *J Hazard Mater*, 2011, 186, 984-990.
55. Y. H. Xiong, Y. M. Qin, L. J. Su and F. G. Ye, *Chem-Eur J*, 2017, 23, 11037-11045.
56. S. F. Wu, Y. Liu, G. P. Yu, J. G. Guan, C. Y. Pan, Y. Du, X. Xiong and Z. G. Wang, *Macromolecules*, 2014, 47, 2875-2882.
57. S. Wu, S. Gu, A. Zhang, G. Yu, Z. Wang, J. Jian and C. Pan, *Journal of Materials Chemistry A*, 2015, 3, 878-885.
58. S. Kuecken, J. Schmidt, L. J. Zhi and A. Thomas, *Journal of Materials Chemistry A*, 2015, 3, 24422-24427.
59. S. J. Ren, M. J. Bojdys, R. Dawson, A. Laybourn, Y. Z. Khimyak, D. J. Adams and A. I. Cooper, *Advanced materials*, 2012, 24, 2357-2361.
60. T. Hasell, S. Y. Chong, K. E. Jelfs, D. J. Adams and A. I. Cooper, *J Am Chem Soc*, 2012, 134, 588-598.
61. A. Bhunia, D. Esquivel, S. Dey, R. Fernandez-Teran, Y. Goto, S. Inagaki, P. Van der Voort and C. Janiak, *Journal of Materials Chemistry A*, 2016, 4, 13450-13457.
62. X. Y. Wang, C. Zhang, Y. Zhao, S. J. Ren and J. X. Jiang, *Macromolecular Rapid Communications*, 2016, 37, 323-329.
63. A. Bhunia, V. Vasylyeva and C. Janiak, *Chem Commun*, 2013, 49, 3961-3963.
64. J. J. Liu, W. Zan, K. Li, Y. Yang, F. X. Bu and Y. X. Xu, *J Am Chem Soc*, 2017, 139, 11666-11669.
65. W. Huang, Z. J. Wang, B. C. Ma, S. Ghasimi, D. Gehrig, F. Laquai, K. Landfester and K. A. I. Zhang, *Journal of Materials Chemistry A*, 2016, 4, 7555-7559.
66. W. Huang, B. C. Ma, H. Lu, R. Li, L. Wang, K. Landfester and K. A. I. Zhang, *Acs Catal*, 2017, 7, 5438-5442.
67. H. Lim, M. C. Cha and J. Y. Chang, *Macromol Chem Phys*, 2012, 213, 1385-1390.
68. P. Puthiaraj, S. M. Cho, Y. R. Lee and W. S. Ahn, *Journal of Materials Chemistry A*, 2015, 3, 6792-6797.
69. P. Puthiaraj, S. S. Kim and W. S. Ahn, *Chem Eng J*, 2016, 283, 184-192.
70. S. H. Xiong, X. Fu, L. Xiang, G. Yu, J. P. Guan, Z. G. Wang, Y. Du, X. Xiong and C. Y. Pan, *Polymer Chemistry*, 2014, 5, 3424-3431.
71. S. K. Das, X. B. Wang and Z. P. Lai, *Micropor Mesopor Mat*, 2018, 255, 76-83.
72. E. Troschke, S. Grätz, T. Lübken and L. Borchardt, *Angewandte Chemie International Edition*, 2017, 56, 6859-6863.
73. S. He, Q. Rong, H. Niu and Y. Cai, *Chem Commun (Camb)*, 2017, 53, 9636-9639.
74. D. Kaleeswaran, R. Antony, A. Sharma, A. Malani and R. Murugavel, *Chempluschem*, 2017, 82, 1253-1265.
75. L. Q. Xu, S. Y. Ding, J. M. Liu, J. L. Sun, W. Wang and Q. Y. Zheng, *Chem Commun*, 2016, 52, 4706-4709.
76. M. G. Schwab, B. Fassbender, H. W. Spiess, A. Thomas, X. L. Feng and K. Mullen, *J Am Chem Soc*, 2009, 131, 7216-7217.
77. W. Zhang, L. G. Qiu, Y. P. Yuan, A. J. Xie, Y. H. Shen and J. F. Zhu, *J Hazard Mater*, 2012, 221, 147-154.
78. A. Halder, S. Kandambeth, B. P. Biswal, G. Kaur, N. C. Roy, M. Addicoat, J. K. Salunke, S. Banerjee, K. Vanka, T. Heine, S. Verma and R. Banerjee, *Angew Chem Int Edit*, 2016, 55, 7806-7810.

79. H. L. Qian, C. Dai, C. X. Yang and X. P. Yan, *ACS applied materials & interfaces*, 2017, 9, 24999-25005.
80. R. Gomes, P. Bhanja and A. Bhaumik, *Chem Commun*, 2015, 51, 10050-10053.
81. R. Gomes and A. Bhaumik, *Rsc Adv*, 2016, 6, 28047-28054.
82. V. Sadhasivam, R. Balasaravanan, C. Chithiraikumar and A. Siva, *Chemistryselect*, 2017, 2, 1063-1070.
83. P. Puthiaraj and K. Pitchumani, *Chem-Eur J*, 2014, 20, 8761-8770.
84. T. T. Liu, X. Y. Hu, Y. F. Wang, L. Y. Meng, Y. N. Zhou, J. X. Zhang, M. Chen and X. M. Zhang, *J Photoch Photobio B*, 2017, 175, 156-162.
85. N. Xu, R. L. Wang, D. P. Li, X. Meng, J. L. Mu, Z. Y. Zhou and Z. M. Su, *Dalton T*, 2018, 47, 4191-4197.
86. X. H. Guo, Y. Tian, M. C. Zhang, Y. Li, R. Wen, X. Li, X. F. Li, Y. Xue, L. J. Ma, C. Q. Xia and S. J. Li, *Chemistry of Materials*, 2018, 30, 2299-2308.
87. A. K. Sekizkardes, S. Altarawneh, Z. Kahveci, T. İslamoğlu and H. M. El-Kaderi, *Macromolecules*, 2014, 47, 8328-8334.
88. J. Liu, K. K. Yee, K. K. W. Lo, K. Y. Zhang, W. P. To, C. M. Che and Z. T. Xu, *J Am Chem Soc*, 2014, 136, 2818-2824.
89. P. Wen, C. Y. Zhang, Z. G. Yang, R. Dong, D. M. Wang, M. J. Fan and J. Q. Wang, *Tribol Int*, 2017, 111, 57-65.
90. S. Gopi and M. Kathiresan, *Polymer*, 2017, 109, 315-320.
91. H. Y. Zhao, Z. Jin, H. M. Su, X. F. Jing, F. X. Sun and G. S. Zhu, *Chem Commun*, 2011, 47, 6389-6391.
92. C. Y. Bai, M. C. Zhang, B. Li, Y. Tian, S. Zhang, X. S. Zhao, Y. Li, L. Wang, L. J. Ma and S. J. Li, *J Hazard Mater*, 2015, 300, 368-377.
93. P. Puthiaraj and K. Pitchumani, *Green Chem*, 2014, 16, 4223-4233.
94. H. A. Patel, F. Karadas, J. Byun, J. Park, E. Deniz, A. Canlier, Y. Jung, M. Atilhan and C. T. Yavuz, *Adv Funct Mater*, 2013, 23, 2270-2276.
95. Y. L. Luo, B. Y. Li, L. Y. Liang and B. E. Tan, *Chem Commun*, 2011, 47, 7704-7706.
96. T. Wang, R. Xue, H. Q. Chen, P. L. Shi, X. Lei, Y. L. Wei, H. Guo and W. Yang, *New J Chem*, 2017, 41, 14272-14278.
97. Y. Z. Liao, J. Weber and C. F. J. Faul, *Macromolecules*, 2015, 48, 2064-2073.
98. X. Zhu, S. H. An, Y. Liu, J. Hu, H. L. Liu, C. C. Tian, S. Dai, X. J. Yang, H. L. Wang, C. W. Abney and S. Dai, *Aiche Journal*, 2017, 63, 3470-3478.
99. A. Modak, M. Pramanik, S. Inagaki and A. Bhaumik, *Journal of Materials Chemistry A*, 2014, 2, 11642-11650.
100. S. Ren, R. Dawson, A. Laybourn, J.-x. Jiang, Y. Khimyak, D. J. Adams and A. I. Cooper, *Polymer Chemistry*, 2012, 3, 928-934.
101. Y. Zhang, A. Sigen, Y. Zou, X. Luo, Z. Li, H. Xia, X. Liu and Y. Mu, *Journal of Materials Chemistry A*, 2014, 2, 13422-13430.
102. Z. Xiang and D. Cao, *Macromolecular rapid communications*, 2012, 33, 1184-1190.
103. Z. Xiang, D. Cao, L. Huang, J. Shui, M. Wang and L. Dai, *Advanced materials*, 2014, 26, 3315-3320.
104. K. Gontarczyk, W. Bury, J. Serwatowski, P. Wiecinski, K. Wozniak, K. Durka and S. Lulinski, *ACS applied materials & interfaces*, 2017, 9, 31129-31141.

105. S. Y. Yu, J. Mahmood, H. J. Noh, J. M. Seo, S. M. Jung, S. H. Shin, Y. K. Im, I. Y. Jeon and J. B. Baek, *Angew Chem Int Edit*, 2018, 57, 8438-8442.
106. M.-S. Kim, C. S. Phang, Y. K. Jeong and J. K. Park, *Polymer Chemistry*, 2017, 8, 5655-5659.
107. K. W. Wang, L. M. Yang, X. Wang, L. P. Guo, G. Cheng, C. Zhang, S. B. Jin, B. Tan and A. Cooper, *Angew Chem Int Edit*, 2017, 56, 14149-14153.
108. M. Liu, Q. Huang, S. Wang, Z. Li, B. Li, S. Jin and B. Tan, *Angewandte Chemie*, 2018, 57, 11968-11972.
109. M. Y. Liu, K. Jiang, X. Ding, S. L. Wang, C. X. Zhang, J. Liu, Z. Zhan, G. Cheng, B. Y. Li, H. Chen, S. B. Jin and B. Tan, *Advanced materials*, 2019, 31, 1807865.
110. M. Dusselier and M. E. Davis, *Chemical reviews*, 2018, 118, 5265-5329.
111. L. J. Kong, J. Zhu, W. Shuang and X. H. Bu, *Adv Energy Mater*, 2018, 8, 1801515.
112. Y. Fu, Z. Q. Wang, S. Z. Li, X. M. He, C. Y. Pan, J. Yan and G. P. Yu, *ACS applied materials & interfaces*, 2018, 10, 36002-36009.
113. L. Hao, S. S. Zhang, R. J. Liu, J. Ning, G. J. Zhang and L. J. Zhi, *Advanced materials*, 2015, 27, 3190-3195.
114. O. Buyukcakir, S. H. Je, S. N. Talapaneni, D. Kim and A. Coskun, *ACS applied materials & interfaces*, 2017, 9, 7209-7216.
115. S. Mukherjee, M. Das, A. Manna, R. Krishna and S. Das, *Chemistry of Materials*, 2019, 31, 3929-3940.
116. K. Wang, H. Huang, D. Liu, C. Wang, J. Li and C. Zhong, *Environmental science & technology*, 2016, 50, 4869-4876.
117. X. Jiang, P. Wang and J. J. Zhao, *Journal of Materials Chemistry A*, 2015, 3, 7750-7758.
118. X. Zhu, C. C. Tian, S. M. Mahurin, S. H. Chai, C. M. Wang, S. Brown, G. M. Veith, H. M. Luo, H. L. Liu and S. Dai, *J Am Chem Soc*, 2012, 134, 10478-10484.
119. X. Liu, H. Li, Y. Zhang, B. Xu, S. A. H. Xin and Y. Mu, *Polymer Chemistry*, 2013, 4, 2445.
120. A. Bhunia, I. Boldog, A. Möller and C. Janiak, *Journal of Materials Chemistry A*, 2013, 1, 14990-14999.
121. S. Hug, M. B. Mesch, H. Oh, N. Popp, M. Hirscher, J. Senker and B. V. Lotsch, *Journal of Materials Chemistry A*, 2014, 2, 5928-5936.
122. S. Dey, A. Bhunia, D. Esquivel and C. Janiak, *Journal of Materials Chemistry A*, 2016, 4, 6259-6263.
123. L. M. Tao, F. Niu, J. G. Liu, T. M. Wang and Q. H. Wang, *Rsc Adv*, 2016, 6, 94365-94372.
124. K. Yuan, C. Liu, J. Han, G. Yu, J. Wang, H. Duan, Z. Wang and X. Jian, *Rsc Adv*, 2016, 6, 12009-12020.
125. S. K. Das, X. Wang, M. M. Ostwal and Z. Lai, *Separation and Purification Technology*, 2016, 170, 68-77.
126. X. Zhu, C. Tian, G. M. Veith, C. W. Abney, J. r. m. Dehaudt and S. Dai, *J Am Chem Soc*, 2016, 138, 11497-11500.
127. K. Park, K. Lee, H. Kim, V. Ganesan, K. Cho, S. K. Jeong and S. Yoon, *Journal of Materials Chemistry A*, 2017, 5, 8576-8582.
128. S. Dey, A. Bhunia, H. Breitzke, P. B. Groszewicz, G. Buntkowsky and C. Janiak, *Journal of Materials Chemistry A*, 2017, 5, 3609-3620.
129. S. Gu, J. Guo, Q. Huang, J. He, Y. Fu, G. Kuang, C. Pan and G. Yu, *Macromolecules*, 2017, 50, 8512-8520.

130. B. Guo, C. Wu, Q. Su, Z. Liu, X. Li, G. Li and Q. Wu, *Materials Letters*, 2018, 221, 236-239.
131. L. Shao, Y. Li, J. Huang and Y.-N. Liu, *Industrial & Engineering Chemistry Research*, 2018, 57, 2856-2865.
132. D. M. D'Alessandro, B. Smit and J. R. Long, *Angewandte Chemie International Edition*, 2010, 49, 6058-6082.
133. K. Yuan, C. Liu, L. Zong, G. Yu, S. Cheng, J. Wang, Z. Weng and X. Jian, *ACS applied materials & interfaces*, 2017, 9, 13201-13212.
134. Y. Zhao, K. X. Yao, B. Teng, T. Zhang and Y. Han, *Energy & Environmental Science*, 2013, 6, 3684-3692.
135. S. Wu, Y. Liu, G. Yu, J. Guan, C. Pan, Y. Du, X. Xiong and Z. Wang, *Macromolecules*, 2014, 47, 2875-2882.
136. M. Sevilla, P. Valle-Vigon and A. B. Fuertes, *Adv Funct Mater*, 2011, 21, 2781-2787.
137. M. G. Rabbani, A. K. Sekizkardes, O. M. El-Kadri, B. R. Kaafarani and H. M. El-Kaderi, *Journal of Materials Chemistry*, 2012, 22, 25409-25417.
138. D. E. Demirocak, M. K. Ram, S. S. Srinivasan, D. Y. Goswami and E. K. Stefanakos, *Journal of Materials Chemistry A*, 2013, 1, 13800-13806.
139. P. Puthiaraj, S.-M. Cho, Y.-R. Lee and W.-S. Ahn, *Journal of Materials Chemistry A*, 2015, 3, 6792-6797.
140. A. Myers and J. M. Prausnitz, *AIChE journal*, 1965, 11, 121-127.
141. S. Hug, L. Stegbauer, H. Oh, M. Hirscher and B. V. Lotsch, *Chemistry of Materials*, 2015, 27, 8001-8010.
142. X. Fu, Y. Zhang, S. Gu, Y. Zhu, G. Yu, C. Pan, Z. Wang and Y. Hu, *Chemistry–A European Journal*, 2015, 21, 13357-13363.
143. M. Saleh, S. B. Baek, H. M. Lee and K. S. Kim, *The Journal of Physical Chemistry C*, 2015, 119, 5395-5402.
144. R. Dawson, A. I. Cooper and D. J. Adams, *Polym Int*, 2013, 62, 345-352.
145. S. K. Das, X. Wang, M. M. Ostwal, Y. Zhao, Y. Han and Z. Lai, *Chemical Engineering Science*, 2016, 145, 21-30.
146. S. K. Das, X. Wang and Z. Lai, *Micropor Mesopor Mat*, 2018, 255, 76-83.
147. S. Dey, A. Bhunia, I. Boldog and C. Janiak, *Micropor Mesopor Mat*, 2017, 241, 303-315.
148. K. Wang, Y. Tang, Q. Jiang, Y. Lan, H. Huang, D. Liu and C. Zhong, *J Energy Chem*, 2017, 26, 902-908.
149. P. M. Mathias, R. Kumar, J. D. Moyer, J. M. Schork, S. R. Srinivasan, S. R. Auvil and O. Talu, *Industrial & engineering chemistry research*, 1996, 35, 2477-2483.
150. Y. J. Lee, S. N. Talapaneni and A. Coskun, *ACS applied materials & interfaces*, 2017, 9, 30679-30685.
151. Y. S. Bae and R. Q. Snurr, *Angew Chem Int Edit*, 2011, 50, 11586-11596.
152. G. Tuci, M. Pilaski, H. Ba, A. Rossin, L. Luconi, S. Caporali, C. Pham‐Huu, R. Palkovits and G. Giambastiani, *Adv Funct Mater*, 2017, 27, 1605672.
153. S. Nandi, U. Werner-Zwanziger and R. Vaidhyanathan, *Journal of Materials Chemistry A*, 2015, 3, 21116-21122.
154. C. Gu, D. Liu, W. Huang, J. Liu and R. Yang, *Polymer Chemistry*, 2015, 6, 7410-7417.
155. A. Modak, M. Pramanik, S. Inagaki and A. Bhaumik, *Journal of Materials Chemistry A*, 2014, 2, 11642-11650.

156. S. M. Kuznicki, V. A. Bell, S. Nair, H. W. Hillhouse, R. M. Jacubinas, C. M. Braunbarth, B. H. Toby and M. Tsapatsis, *Nature*, 2001, 412, 720-724.
157. G. Wang, K. Leus, S. Zhao and P. Van Der Voort, *ACS applied materials & interfaces*, 2017, 10, 1244-1249.
158. J. C. Wang and S. Kaskel, *Journal of Materials Chemistry*, 2012, 22, 23710-23725.
159. J. Liu, X. Liu, Y. Sun, C. Sun, H. Liu, L. A. Stevens, K. Li and C. E. Snape, *Advanced Sustainable Systems*, 2018, 2, 1700115.
160. P. Puthiaraj and W.-S. Ahn, *J Energy Chem*, 2017, 26, 965-971.
161. K. K. Wang, H. L. Huang, D. H. Liu, C. Wang, J. P. Li and C. L. Zhong, *Environmental Science & Technology*, 2016, 50, 4869-4876.
162. Z. Z. Yang, S. Wang, Z. H. Zhang, W. Guo, K. C. Jie, M. I. Hashim, O. S. Miljanic, D. E. Jiang, I. Popovs and S. Dai, *Journal of Materials Chemistry A*, 2019, 7, 17277-17282.
163. S. Mukherjee, M. Das, A. Manna, R. Krishna and S. Das, *Journal of Materials Chemistry A*, 2019, 7, 1055-1068.
164. M. R. Liebl and J. Senker, *Chemistry of Materials*, 2013, 25, 970-980.
165. Y. Fu, Z. Wang, X. Fu, J. Yan, C. Liu, C. Pan and G. Yu, *Journal of Materials Chemistry A*, 2017, 5, 21266-21274.